Computation of electroconductive gyrotactic bioconvection from a nonlinear inclined stretching sheet under non-uniform magnetic field : simulation of smart bio-nano-polymer coatings for solar energy

Beg, OA, Aneja, M, Sharma, SAPNA and Kuharat, S

http://dx.doi.org/10.1142/S0217979220500289

INTERNATIONAL JOURNAL OF MODERN PHYSICS B

(Condensed Matter Physics; Statistical Physics; Atomic, Molecular and Optical Physics)
ISSN (print): 0217-9792 | ISSN (online): 1793-6578

IN PRESS, FEBRUARY 11TH 2020

COMPUTATION OF ELECTRO-CONDUCTIVE GYROTACTIC BIOCONVECTION FROM A NONLINEAR INCLINED STRETCHING SHEET UNDER NON-UNIFORM MAGNETIC FIELD: *SIMULATION OF SMART BIO-NANO-POLYMER COATINGS FOR SOLAR ENERGY*

M. Aneja*, Sapna Sharma*, Sireetorn Kuharat ** and **O. Anwar Bég****

School of Mathematics, Thapar University, Patiala - 147001,* ***India*

*** Aeronautical and Mechanical Engineering, SEE, University of Salford, Manchester, M54WT,* ***UK***

ABSTRACT

Incompressible, steady-state, boundary layer magneto-bioconvection of a nanofluid (containing motile gyrotactic micro-organisms) over a nonlinear inclined stretching sheet subjected to non-uniform magnetic field is studied theoretically and numerically. This regime is encountered in novel bio-nano-material electroconductive polymeric processing systems currently being considered for third generation organic solar coatings, anti-fouling marine coatings etc. Buongiorno's two-component nanofluid model is deployed with the Oberbeck-Boussinesq approximation. Ohmic dissipation (Joule heating) is included. The governing nonlinear partial differential equations are reduced to a system of ordinary differential equations and appropriate similarity transformations. The normalized system of equations with associated boundary conditions features a number of important dimensionless parameters including magnetohydrodynamic body force parameter (M), sheet inclination (δ), Brownian motion nanoscale parameter (Nb), thermophoresis nanoscale parameter (Nt), Richardson number ($Ri=GrRe^2$, where Gr is thermal Grashof number and Re is Reynolds number), buoyancy ratio parameter (Nr), Eckert (viscous dissipation) number (Ec), bioconvection Rayleigh number (Rb), Lewis number (Le), bioconvection Lewis number (Lb), Péclet number (Pe), nonlinear stretching parameter (n) are solved with a variational Finite Element Method (**FEM**). Validation is conducted with earlier published studies of Khan and Pop (2010) for the case of non-magnetic stretching sheet nanofluid flow without bioconvection. Further validation of the general magnetic bioconvection nanofluid model is achieved with a generalized differential quadrature (**GDQ**) numerical technique developed by Bég and Kuharat (2017). The response of non-dimensional velocity, temperature, nanoparticle concentration, motile micro-organism density function, local skin friction coefficient, Nusselt number, Sherwood number, wall motile density gradient function to variation in physically pertinent values of selected control parameters (representative of real solar bio-nano-magnetic materials manufacturing systems) are studied in detail. Interesting features of the flow dynamics are elaborated and new future pathways for extension of the study identified in bio-magneto-nano polymers (BMNPs) for solar coatings.

KEYWORDS: *Bioconvection, Nanofluid, Gyrotactic micro-organisms, Magnetic field, Brownian motion, Thermophoresis; Bio-magneto-nano-polymers; solar coatings; numerical; finite element method; generalized differential quadrature; Viscous and Joule heating.*

NOTATION:

b	chemotaxis constant
C	nanoparticle concentration
C_{fx}	local Skin friction coefficient
D_B	Brownian diffusion coefficient
D_m	motile micro-organism diffusivity
D_T	thermophoresis diffusion coefficient
Ec	Eckert number
$f(\eta)$	non-dimensional stream function
g	acceleration due to gravity
Gr/Re^2	local Richardson number (in terms of Grashof and Reynolds numbers)
k	thermal conductivity of fluid
Lb	bioconvection Lewis number
Le	Lewis number
N	density of motile micro-organisms
n	nonlinear sheet stretching parameter
N_{nx}	local density number of the motile micro-organisms
N_{ux}	local Nusselt number
Nb	Brownian motion parameter
Nr	buoyancy ratio parameter
Nt	thermophoresis parameter
P	Pressure
Pe	bioconvection Péclet number
Pr	Prandtl number
q_m	wall mass flux
q_n	wall motile micro-organism flux
q_w	wall heat flux
Rb	bioconvection Rayleigh number
Re_x	local Reynolds number

Sh_x	local Sherwood number
T	temperature
u,v	x,y velocity components
W_c	maximum cell swimming speed
$( )_w$	wall conditions
$( )_\infty$	free stream conditions

Greek

α	thermal diffusivity (= $k\,\rho Cp$)
δ	angle of inclination of stretching sheet
γ	average volume of motile micro-organisms
Ω	motile micro-organisms concentration difference parameter
ρ_f	density of nanofluid
ρ_m	density of motile micro-organisms
ρ_p	density of nanoparticles
σ	electrical conductivity
τ	ratio of effective heat capacitance (= $(\rho C)_p/(\rho C)_f$)
η	non-dimensional transverse coordinate
$\theta(\eta)$	non-dimensional temperature function
$\phi(\eta)$	non-dimensional nano-particle concentration function
$\chi(\eta)$	non-dimensional motile micro-organism density function

1.INTRODUCTION

In recent years there has been a concerted effort in fusing together nano- nanotechnology and microbiology to develop more robust materials for engineering applications. For example, in solar coating materials, greater emphasis has been placed on designing **s**ustainable, clean, durable and ecologically friendly coating materials. inexpensive power systems. Although significant progress has been made in refining the working fluids in solar collectors via nano-particle doping, only recently have engineers focused on revolutionizing the coating materials for solar cells and photovoltaics. Among the most promising of these developments i**s** *organic solar paint*. This environmentally-friendly technology takes the form of coatings or flexible

polymeric sheets that are precision-designed to contain a nano-particle fluid that is essentially water-based paint. The presence of the nano-particles has been confirmed to enhance durability, anti-corrosion and anti-abrasion characteristics of solar coatings which may be regarded as smart thermochromic materials [1, 2]. These materials may also be electrically-conducting i.e. magnetized. As such *electro-conductive polymeric solar materials* (e.g. magnetized sol gels) can lead to a more consistent and predictable power output and sustained efficiency. These coating protects the glass from erosion, and from stubborn staining from salt and mineral deposits and furthermore have confirmed properties which can permit efficient performance in harsh environmental conditions from sub-zero to extreme hot environments. Solar gel coated systems constitute third generation solar designs (organic polymer-based nano-coatings) which are superceding the earlier first generation (silicon-based) and second generation (thin film) solar cells. The parallel developments in biomimetics and exploiting biological phenomena for technological designs has also led to interest in embedding micro-organisms in certain coatings. Bacterial micro-organisms have tremendous anti-fouling properties and also protect engineering surfaces from environmental contamination. The resulting materials are sometimes called biofunctional materials [3]. Functional surfaces with UV or visible light–active photocatalyst content can circumvent environmental degradation due to photocatalytic properties. Due to these properties, a wide range of pathogen bacteria can be inactivated under visible light illumination. When nano-doping, magnetic properties and embedded micro-organisms are combined a new generation of solar coatings is achieved, namely *magneto-nano-bio-coatings* [4]. The fundamental basis for nano-coatings (whether magnetic or biologically modified) is *nanofluid science and technology*. Introduced by Argonne energy laboratory pioneers, Choi and Eastman [5] in the 1990s, a nanofluid is a suspension of nano-sized particles (usually metallic) introduced into a base fluid (water, ethylene glycol, air, lubricant etc) which boosts the effective thermal conductivity of the composite medium and even at relatively low volume fractions, the heat transfer enhancement is considerable. Via strategic dispersion of nanoparticles in the base fluid, it has been shown that addition of less than 1% of nanoparticles doubles the heat conductivity of the nanofluid, as noted by Choi and Eastman [5] and Das *et al.* [6]. Many analytical and computational studies of nanofluid dynamics have been communicated in the last decade or so. These have included external boundary layer flows, internal developing flows, swirling flows, squeezing flows, wedge (Falkner-Skan flows), peristaltic pumping, magnetohydrodynamics and helical flows. Many of these works have been reviewed recently by Bég [7]. The vast majority of these studies deploy either the *Buongiorno two-component model* (which invokes a species diffusion

equation for nano-particles) [8] or the simpler *Tiwari-Das model* [9] (which allows volume fraction and different nanofluid properties to be simulated). A particular category of flows of special relevance to nanomaterial coating dynamics processes is *stretching sheet flow*. This sub-set of manufacturing fluid dynamics is an intriguing multi-physics problem. It combines magnetohydrodynamics, nanofluid dynamics, bioconvection phenomena and other thermal physics aspects. Several authors have investigated magnetic nanofluid flows from stretching surfaces. The presence of simultaneous heat and mass transfer also adds significant complexity. Owing to the inherent nonlinearity in such systems, numerical methods are the usual approach for solving the strongly coupled, nonlinear ordinary or partial differential boundary value problems arising in these types of flows. Magnetic nanofluid dynamics involves a considerable range of electromagnetic phenomena including magnetic induction, combined electrical and magnetic fields, steady and transient electromagnetic fields, Ohmic dissipation, Hall currents, ionslip currents, Maxwell displacement currents etc. Relevant studies include Ibrahim and Shankar [10] who considered slip magnetic nanofluid stretching sheet flow with suction. Rana *et al.* [11] who presented finite element solutions for time-dependent magnetized rotating stretching sheet nanofluid flow. Rana and Bég [12] obtained numerical solutions for multiple nanoscale geometric and thermophysical effects on oblique mixed convection hydromagnetic nanofluid flow. Bég *et al.* [13] used an optimized Crank-Nicolson finite difference method to simulate permeability and strong magnetic field effects on transient magneto-nanofluid flow from an exponentially stretching sheet in porous media. Ferdows *et al.* [14] investigated thermal radiative flux and wall blowing effects on unsteady magnetic nano-polymer stretching sheet flow. Mansur *et al.* [15] investigated stagnation point dynamics in magnetic nanofluid flow from expanding/contracting sheets with wall transpiration. Further studies include Ibrahim [16] (with magnetic induction), Thumma *et al.* [17] (with heat generation/absorption effects), Hayat *et al.* [18] (for rheological nanofluids), Zohra *et al.* [19] (for dual electrical and magnetic fields in Falkner-Skan nanofluid boundary layers), Bég *et al.* [20] (various metallic nano-particles in solar magnetic nano-polymer stretching sheet coating flows e.g. silver and titanium oxide) and Bég *et al.* [21] (for thermo-capillary inductive magnetic nanofluid stretching sheet fabrication flows).

As elaborated earlier, numerous modern solar coatings are amalgamating the properties of bacterial micro-organisms with nano-doping of materials. The specific type of bacterial micro-organism deployed can have profound effects on the constitution of the synthesized magnetic bio-nano-materials. Micro-organisms can be thermophilic, photo-phylic etc. Many excellent

studies have been conducted in recent years examining various combinations of metallic nano-particles and micro-organisms. Pertinent work in this area includes Órdenes-Aenishanslins *et al.* [22] (on titanium dioxide nanoparticles biosynthesized by *Bacillus mycoides* in solar cells), Fayaz *et al*. [23] (on biomanufacturing of silver and gold nanoparticles using thermophilic bacterium *Geobacillus stearothermophilus*for solar coating sheets), Saxena *et al.* [24] (on silver nanoparticles with *Ficus benghalensis* botanical bacterial micro-organisms), Kirthi et al. [25] (on biosynthesis of titanium dioxide nanoparticles using bacterium *Bacillus subtilis*). Other interesting experimental investigations include Jha *et al*. [26] and Dhandapani *et al.* [27] (for fabrication of titanium dioxide nanoparticles and deployment in solar aquatic bio-coatings), Klaus-Joerger *et al*. [28] (on design of chemically-modified metallic nano-particles for biological ceramic–metal (cermet) structured coatings), Narayana and Sakthivel [29], Schröfel *et al.* [30] (on novel "bottom-up" biofabrication methods for combined bioconvetive micro-organisms and biosynthesized metallic nanoparticles) and Sadowski *et al.* [31] (on photoelectrochemical manipulation of bacteria embedded in nanofluid titanium dioxide organic solar polymers). One of the many mechanisms responsible for bacterial trans-location is *bioconvection* which refers to the phenomenon of *macroscopic convective motion of fluid caused by a density gradient* and is created by collective swimming of motile micro-organisms e.g. bacteria. The density of base fluid increases as these self-propelled motile micro-organisms swim in a particular direction, thus generating bioconvection patterns [32, 33]. Simple mathematical models for hydrodynamics of bioconvection patterns due to motile micro-organisms have been presented by Pedley *et al*. [34], although without any consideration of engineering applications. The motile microorganisms may be classified as *oxytactic, chemotactic, negative gravitactic, gyrotactic, magneto-tactic* or *photo-tactic* depending on the stimulus which induces motion. The stimulators of these six broad categories of micro-organisms are oxygen concentration gradient, chemical species (e.g. acidity), negative gravity, torque (i.e. displacement between the center of buoyancy and mass), magnetic fields or light, respectively [35]. There is dissimilarity between micro-organism and nanoparticle dynamics. Micro-organisms are *self-propelled* whereas nanoparticles are driven by Brownian motion and thermophoresis. It is thus perceptible that motion of the motile micro-organisms is independent of the motion of nanoparticles. For micro-organisms to survive in the base fluid, the nanofluid has to be *water-based*. There are many applications of bioconvection in bio-microsystems engineering including enzyme biosensors [36], chip-size micro-devices for evaluating nanoparticle toxicity [37] and design of the critical functional alveolar-capillary interface of the human lung to evaluate toxic and inflammatory responses of the lung to silica nanoparticles

[38]. The first attempt at developing a viscous fluid dynamic model for *combined nanofluid bioconvection* was presented by Kuznetsov [39] who analysed with a perturbation method the stability of bioconvection in a horizontal layer filled with a base fluid containing both gyrotactic micro-organisms and also nanoparticles. In this study the Buongiorno nanoscale model [8] was used i.e. specific metallic nano-particles *were not* considered. Boundary layer flow studies of nanofluids were initiated by Kuznetsov and Nield [40]. Later Aziz *et al.* [41] extended the Kuznetsov-Nield model to bioconvection. Subsequently many other studies have been communicated. These have invariably taken the form of *non-linear computational boundary value problems* aimed at determining engineering characteristics e.g. heat transfer rate, wall nano-particle species gradient, motile micro-organism density gradient etc. Khan *et al.* [42] studied the influence of Navier slip and magnetic field on the heat and mass transfer of a nanofluid containing gyrotactic microorganisms from a vertical surface. Uddin *et al.* [43] employed a collocation numerical method to simulate amplitude characteristics in oxytactic bioconvection nanofluid slip heat and mass transfer from a wavy surface. Latiff *et al.* [44] used Maple quadrature to derive computational solutions for time-dependent forced micropolar nanofluid bioconvection slip from a stretching/ shrinking sheet by amalgamating the Eringen micro-morphic rheological model with the Buongiorno-Kuznetsov nanofluid gyrotactic model. Das *et al.* [45] analyzed the two-dimensional chemically-reactive nanofluid gyrotactic bioconvection in permeable material. Shaw *et al.* [46] analyzed cross-diffusion effects in hydromagnetic bioconvective gryotactic nanofluid flow. Zhao *et al.* [47] examined transient MHD reactive bio-nanofluid lubrication. Bég *et al.* [48] used spectral methods to model the oxytactic bioconvective nanofluid flow in a deformable nanofuel cell. Further studies include Mutuku and Makinde [49], Bég *et al.* [50] on rheological biconvection nanofluid dynamics in near-wall biomaterials processing, Li *et al.*, [51] in unsteady dual disk intercalated squeeze film mixed bioconvection nanofluid films. In many of these studies the excellent control mechanism offered by external applied magnetic fields in manipulating properties of magnetic nano-biconvection suspensions has been confirmed. The flow kinematics can be altered to control better the rate of solidification, nano-particle diffusion rates, dispersion and intensity of micro-organism propulsion and localization. However, in the studies described generally only constant, static magnetic field has been simulated. However non-uniform magnetic fields also arise in materials synthesis operations and incorporation of this feature provides a more realistic model, as elaborated by Zhang and Zhao [52]. Further corroboration of this in the context of solar magnetic nano-materials/fluids has been provided by Xu *et al.* [53]. An inspection of the literature shows that very sparse attention has been directed thusfar at simulating magnetized

nanofluid bioconvection coating flows from a stretching surface in the presence of a a non-uniform magnetic field. Mehyran *et al.* [54] have considered this problem albeit for the case of a vertical stretching sheet and in the absence of viscous dissipation.

The current article generalizes the study in [54] to consider gyrotactic bioconvection nanofluid magnetized boundary layer flow from an *inclined* non-linear stretching surface *in the presence of significant viscous dissipation and Ohmic dissipation (Joule heating).* The inclination of the fabrication surface permits the scaling of gravity effects which provide a further mechanism of controlling the magnetic bio-nano-materials processing operations. Dissipation has been shown to be a significant phenomenon even in low-speed incompressible heat transfer systems featuring buoyancy effects, as elucidated by Gebhart. [55]. It is also important in solar nano-coating synthesis operations as elaborated by Alghoul *et al.* [56] and Charitidis *et al.* [57]. Several authors have considered magnetic nanofluid dynamics flows with viscous heating (dissipation) including Thumma *et al*. [58] (for rotating fabrication systems), Shukla *et al.* [59] for enrobing of cylinders and Nayak *et al.* [60] for contracting sheet radiative convection flows. However, to the authors' knowledge no study has thus far examined the collective effects of viscous heating and sheet inclination on magnetic bioconvection nanofluid dynamics. In the present work the governing conservation equations (based on the Buongiorno-Kuznetsov gyrotactic nanofluid model) are converted from nonlinear partial differential equations are converted via similarity transformations to a ninth order, coupled, nonlinear system of ordinary differential equations. The emerging boundary value problem is solved by an efficient variational finite element method. Numerical results for various physical parameters are expressed graphically and discussed. Validation with previous studies for two special cases i.e. negating bioconvection and viscous heating and sheet inclination, respectively, is conducted. Further verification of the general model solutions with the generalized differential quadrature (**GDQ**) method [61] is included.

2. MATHEMATICAL MODEL

Let us consider two-dimensional, steady, laminar, incompressible, viscous boundary layer flow of electrically-conducting nanofluid containing gyrotactic micro-organisms from a nonlinear stretching sheet which is inclined from the vertical with an acute angle δ. The physical model of the problem and cartesian coordinates is shown in **Fig 1**. The x-direction is taken along the leading edge of the inclined stretching sheet and the *y*-direction is normal to it. Water is considered as base fluid and this allows the proliferation of thermophile gyrotactic micro-

organisms. Following Mehyran *et al.* [54] and Chiam [62] the sheet is stretched with a power-law velocity i.e. stretching velocity $u_w = ax^n$ where a is a positive constant and n is termed the *nonlinear stretching parameter*. A variable intensity magnetic field $B(x) = B_o x^{(n-1)/2}$ is applied in the direction parallel to the y-axis. Joule heating (Ohmic dissipation) is included. However induced magnetic is negligible compared to external magnetic field. The nanofluid suspension is dilute since there is no agglomeration and accumulation of nanoparticles i.e. homogenous dispersion is achieved. Additionally, implicit to the model is the assumption that nanoparticles have no effect on the direction and velocity of gyrotactic micro-organisms swimming. The Boussinesq approximation is used to determine the variation of density in the buoyancy term. Viscous dissipation is included and the base fluid (water-based solar coating) and nanoparticles are in a state of thermal equilibrium. Moreover, motile micro-organisms, nanoparticles and base fluid have similar velocity, following Khan *et al.* [42]. Under these approximations, the governing conservation equations for mass, momentum, energy (heat), nano-particle species concentration and motile micro-organism density conservation, may be shown to take the form:

Mass:

$$\frac{\partial u}{\partial x} + \frac{\partial v}{\partial y} = 0 \tag{1}$$

$\boldsymbol{x - Momentum}$:

$$\rho f\left(u\frac{\partial u}{\partial x} + v\frac{\partial v}{\partial y}\right) = -\frac{\partial p}{\partial x} + u_f\left(\frac{\partial^2 u}{\partial x} + \frac{\partial^2 u}{\partial y^2}\right) + \rho_f g\beta(1 - C_\infty)(T - T_\infty)cos\delta - g\left(\rho_p - \rho_f\right)(C - C_\infty)cos\delta - gy\left(\rho_m - \rho_f\right)(N - N_\infty)cos\delta - \sigma B^2(x)u \tag{2}$$

$\boldsymbol{y - Momentum}$:

$$\frac{\partial P}{\partial y} = 0 \tag{3}$$

Energy:

$$u\frac{\partial T}{\partial x} + v\frac{\partial T}{\partial y} = \alpha\left(\frac{\partial^2 T}{\partial x^2} + \frac{\partial^2 T}{\partial y^2}\right) + \tau\left\{D_B\frac{\partial C}{\partial y}\frac{\partial T}{\partial y} + \frac{D_T}{T_\infty}\left(\left(\frac{\partial T}{\partial x}\right)^2 + \left(\frac{\partial T}{\partial y}\right)^2\right)\right\} + \frac{\mu\alpha}{k}\left(\frac{\partial u}{\partial y}\right)^2 + \frac{\sigma\alpha B^2(x)u^2}{k} \tag{4}$$

Nano-particle species concentration:

$$u\frac{\partial C}{\partial x}+v\frac{\partial C}{\partial y}=\alpha\left(\frac{\partial^2 C}{\partial x^2}+\frac{\partial^2 C}{\partial y^2}\right)+\frac{D_T}{T_\infty}\left(\frac{\partial^2 T}{\partial x^2}\frac{\partial^2 T}{\partial y^2}\right) \quad (5)$$

Gyrotactic micro-organism conservation:

$$u\frac{\partial N}{\partial x}+v\frac{\partial N}{\partial y}+\frac{bW_c}{(C_w-C_\infty)}\left[\frac{\partial}{\partial x}\left(N\frac{\partial C}{\partial x}\right)+\frac{\partial}{\partial y}\left(N\frac{\partial C}{\partial y}\right)\right]=D_m\left(\frac{\partial^2 N}{\partial x^2}+\frac{\partial^2 N}{\partial y^2}+2\frac{\partial^2 N}{\partial xy}\right) \quad (6)$$

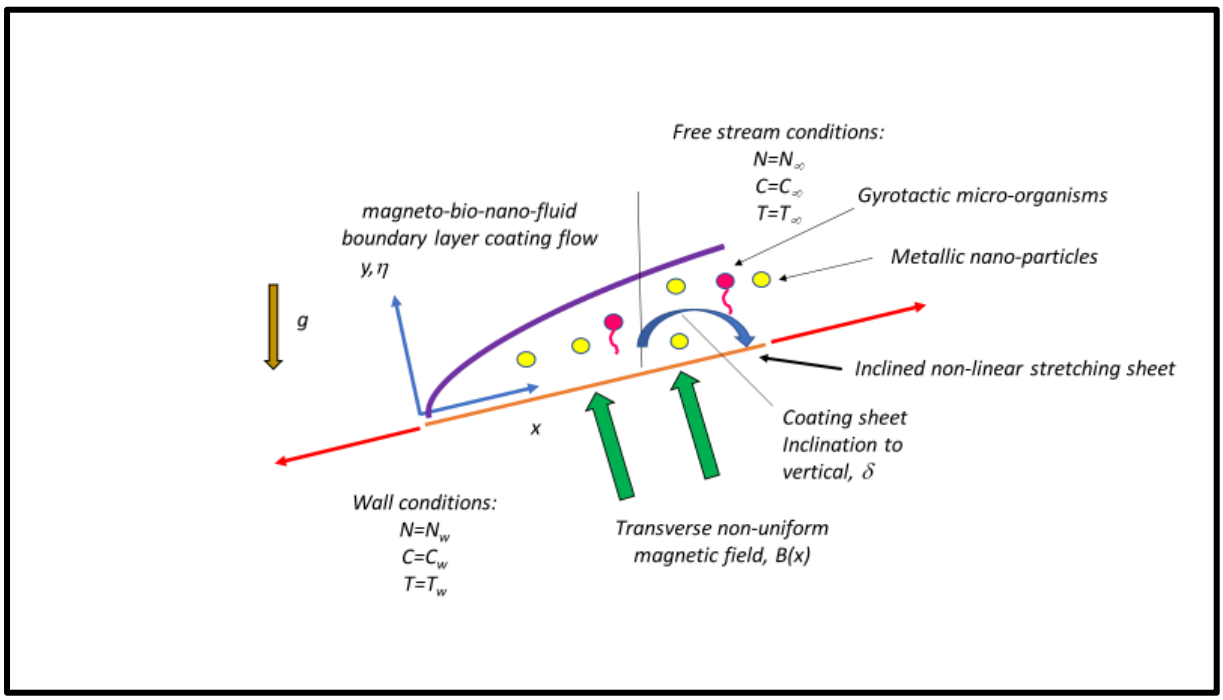

Figure 1: Physical model for solar magneto-bio-nano coating manufacturing simulation

The pressure terms cam be eliminated from Eqns. (2) and (3) by cross differentiation. Integrating the resulting equation with respect to *y* and using the boundary condition at infinity we get:

$$\rho f\left(u\frac{\partial u}{\partial x}+v\frac{\partial v}{\partial y}\right)=u_f\left(\frac{\partial^2 u}{\partial x}+\frac{\partial^2 u}{\partial y^2}\right)+\rho_f g\beta(1-C_\infty)(T-T_\infty)cos\delta-g\left(\rho_p-\rho_f\right)(C-C_\infty)cos\delta-gy\left(\rho_m-\rho_f\right)(N-N_\infty)cos\delta-\sigma B^2(x)u \quad (7)$$

Physically viable boundary conditions for the velocity, temperature, nanoparticle concentration and density of motile micro-organisms are enforced as follows:

$$u=ax^2,\qquad v=0,\qquad T=T_w,\qquad C=C_w,\qquad N=N_w\qquad at\ x=0$$

$$u \to 0, \qquad v \to 0, \qquad T \to T_\infty, \qquad C \to C_\infty, \quad N \to N_\infty \qquad at\ x \to \infty \tag{8}$$

To facilitate numerical solutions, the following similarity variables are introduced [63, 64]:

$$n = y\sqrt{\frac{a(n+1)}{2y}}x^{\frac{(n-1)}{2}}, \qquad u = ax^n f'(n), \qquad v = -\sqrt{\frac{a(n+1)}{2y}}x^{\frac{(n-1)}{2}}\left(f(\eta) + \frac{(n-1)}{(n+1)}\eta f'(\eta)\right),$$
$$\theta(\eta) = \left(\frac{T-T_\infty}{T_w-T_\infty}\right), \qquad \emptyset(\eta) = \left(\frac{C-C_\infty}{C_w-C_\infty}\right), \qquad x(\eta) = \frac{N-N_\infty}{N-N_\infty} \tag{9}$$

The partial differential conservation equations are thereby converted into the following ninth order multi-degree system of nonlinear, coupled and ordinary differential equations which take the form:

$$f''' + ff'' - \left(\frac{2n}{n+1}\right)(f')^2 - Mf' + \left(\frac{2}{n+1}\right)\left(\frac{Gr}{Re^2}\right)(\theta cos\delta - Nrcos\delta - Rb\chi cos\delta) = 0 \tag{10}$$

$$\frac{1}{Pr}\theta'' + \theta'(f + Nb\phi') + Nt(\theta')^2 + Ec[(f'')^2 + 2M(f')^2] = 0 \tag{11}$$

$$\phi'' + Lef\phi' + \left(\frac{Nt}{Nb}\right)\theta'' = 0 \tag{12}$$

$$x'' + Lbfx' - Pe[\phi''(\Omega + \chi) + \phi' x'] = 0 \tag{13}$$

Where $(\ )'$ designates differentiation with respect to the transformed transverse coordinate, η. The parameters arising in Eqns. (10)-(13) are defined as follows:

$$Nb = \frac{\tau D_B(C_w-C_\infty)}{\alpha}, \quad Nt = \frac{\tau D_B(T_w-T_\infty)}{\alpha T_\infty}, \quad M = \frac{2\sigma B_0^2}{ap(n+1)}, \quad \frac{Gr}{Re^2} = \frac{(g\beta(1-C_\infty)(T_w-T_\infty)x^3/v^2)}{u_w^2 x^2/v^2}$$

$$Nr = \frac{(\rho_p - \rho_f)(C_w - C_\infty)}{\rho\beta(1-C_\infty)(T_w - T_\infty)}, \quad Rb = \frac{\gamma(\rho_m - \rho_f)(N_w - N_\infty)}{\rho\beta(1-C_\infty)(T_w - T_\infty)}, \quad Pr = \frac{\nu}{\alpha}, \quad Le = \frac{\nu}{D_B},$$
$$Lb = \nu/D_m, Ec = \frac{u_w^2}{c_p(T_w-T_\infty)}, \quad Pe = \frac{bW_c}{D_m}, \quad \Omega = \frac{N_\infty}{(N_w-N_\infty)}. \tag{14}$$

Here all parameters have been defined in the notation section.

The boundary conditions of equations in similarity space can be written as

$$f(0) = 0, \quad f'(0) = 1, \quad \theta(0) = 1, \quad \chi(0) = 1,$$

$$f'(\infty) = 0,\ \ \theta(\infty) = 0,\ \ \emptyset(\infty) = 0,\ \ \chi(\infty) = 0 \qquad (15)$$

Here again the primes denote differentiation with respect to similarity variable. In solar coating and other magnetic materials processing operations [52], key engineering design parameters include the sheet surface *shear stress, the local heat flux, the local mass flux* and the *motile micro-organisms flux*. These are denoted respectively as τ_w, q_w, q_m and q_n and can be expressed mathematically as follows:

$$T_w = u\left(\frac{\partial u}{\partial y}\right)_{y=0}, q_w = -k\left(\frac{\partial T}{\partial y}\right)_{y=0}, q_m = -D_B\left(\frac{\partial C}{\partial y}\right)_{y=0}, q_n = -D_m\left(\frac{\partial N}{\partial y}\right)_{y=0} \qquad (16)$$

In n*on-dimensional* variables, these design quantities of physical interest are defined as the *skin friction coefficient C_{fx}, the local Nusselt number N_{ux}, the local Sherwood number $Sh_x$and the local density number of the motile micro-organisms N_{nx}* which take the form:

$$C_{fx} = \frac{\tau_w}{\rho u_w^2}, Nu_x = \frac{xq_w}{k(T_w - T_\infty)}, sh_x = \frac{xq_m}{D_B(C_w - C_\infty)}, Nn_x = \frac{xq_n}{D_m(N - N_\infty)} \qquad (17)$$

Eqns. (17) effectively assume the following forms:

$$Re_x^{\frac{1}{2}} C_{fx} = \sqrt{\frac{n+1}{2}} f''(0), \quad Re_x^{\frac{1}{2}} N_{ux} = \sqrt{\frac{n+1}{2}} \theta'(0),$$

$$Re_x^{1/2} Sh_x = \sqrt{\frac{n+1}{2}} \emptyset'(0), \ \ Re_x^{1/2} Nn_x = \sqrt{\frac{n+1}{2}} \chi'(0) \qquad (18)$$

In the above equations, $Re_x = \frac{U_0 x}{\nu}$ refers to the local Reynolds number. The quantities in Eqn. (18) are termed "reduced" quantities as they feature local Reynolds numbers on the left-hand sides.

3. FINITE ELEMENT NUMERICAL SOLUTIONS

The system of nonlinear ordinary differential Eqns. (10)-(13) subjected to boundary conditions (15), which characterizes the solar magnetized bioconvection nanofluid coating regime, has been solved numerically by the variational finite element method. The reduced momentum Eq. (9) is a third order differential equation and is coupled with the heat and nanoparticle

concentration equations via buoyancy terms and also the motile micro-organism density conservation number via advection-diffusion terms. It is therefore judicious to solve these equations in the coupled form. The finite element methodology is well-established and therefore not repeated here. Readers are referred to Bhargava *et al.* [65], 66] for further elaboration of the interpolation weighting functions and stiffness matrix formulations. In summary, firstly the third order momentum equation is reduced to second order via a simple substitution:

$$f' = h. \tag{19}$$

The overall ordinary differential boundary value problem contracts therefore to:

$$h" = fh' - \left(\frac{2n}{n+1}\right)(h)^2 - Mh + \left(\frac{2}{n+1}\right)\left(\frac{Gr}{Re^2}\right)(\theta\cos\delta - Nr\phi\cos\delta\, Rb\chi\cos\delta) = 0 \tag{20}$$

$$\frac{1}{Pr}\theta" + \theta'(f + Nb\phi') + Nt(\theta')^2 + Ec[(h')^2 + M(h)^2] = 0 \tag{21}$$

$$\phi + \mathrm{Lef}\phi' + \left(\frac{\mathrm{Nt}}{\mathrm{Nb}}\right)\theta" = 0 \tag{22}$$

$$\chi" + Lbf\chi' - Pe[\phi"(\Omega + \chi) + \phi'\chi'] = 0 \tag{23}$$

The corresponding boundary conditions (15) reduces to:

$$f(0) = 0, \quad h(0) = 1, \quad \theta(0) = 1, \quad \phi(0) = 1, \quad \chi(0) = 1,$$
$$h(\infty) = 0, \quad \theta(\infty) = 0, \quad \phi(\infty) = 0, \quad \chi(\infty) = 0 \tag{24}$$

The whole finite element domain is divided into 80 two-node line elements, over each of the element, finite element equations are derived. The error tolerance has been considered to be 10^{-4}. The choice of $\eta_\infty = 7$ satisfies the boundary layer conditions i.e. achieves asymptotically smooth results in the free stream. If η_∞ exceeds 7, all the unknown functions do not change up to the desired accuracy. Mesh independence test were also conducted. 80 elements were found to achieve good accuracy with further mesh refinement having no impact on the accuracy. Extensive computations have been performed to investigate the parametric effects on the heat/mass/momentum characteristics of the regime. These are described in due course.

4.VALIDATION WITH PUBLISHED STUDIES AND GDQ METHOD

For the validation of code, a two-tier approach is used. Firstly, a careful comparison with special cases of the general model is conducted. **Table 1 s**hows the benchmarking of the present finite element solutions for reduced Nusselt number with the earlier studies of Khan and Pop [67] for the case where bioconvection is ignored (*Rb = Pe. = Lb = Ω = N r = 0), the sheet is vertical (δ = 0°), linear sheet stretching velocity is assumed (n = 1), magnetic field and viscous heating and Joule dissipation terms vanish (M=Ec =0) but nano-particle effects are retained (Le =10) and Nb≠0 and Nt ≠0).* With these values prescribed in the general model and removal of the micro-organism density number boundary conditions, the boundary value problem reduced exactly to that studied by Khan and Pop [67]. Excellent correlation is achieved between the variational finite element code and the numerical shooting quadrature computations of Khan and Pop [67] for all values of Brownian motion parameter (*Nb*) and thermophoresis parameter (*Nt*).

Table 1: Comparison of results for reduced Nusselt number $\sqrt{\frac{n+1}{2}}\theta'(0)$, for *Le = 10, n = 1, M =Ec = Nr = Rb = Pe = Lb = Ω = 0, δ = 0°* and different values for *Nt and Nb*.

	Nb = 0.1		**Nb = 0.3**		**Nb = 0.3**	
Nt	Present code	Khan and Pop [67]	Present code	Khan and Pop [67]	Present Code	Khan and Pop [67]
0.1	0.956638	0.952493	0.256755	0.2522	0.05596	0.0543
0.2	0.69398	0.6932	0.181657	0.1816	0.0394372	0.0390
0.3	0.524139	0.5201	0.131437	0.1355	0.0299327	0.0291
0.4	0.408426	0.4026	0.100644	0.1046	0.0221499	0.0225
0.5	0.32752	0.3211	0.08291	0.0833	0.0175823	0.0179

Table 2 documents the comparison with Mehryan *et. al*. [54] for density gradient of motile micro-organisms. With *Ec = 0* (negligible viscous heating effect and Ohmic dissipation term ignored in the energy Eqn. (11)) and *δ = 0°* (vertical sheet scenario) the present general model reduces exactly to that solved in [54]. Inspection of the table reveals that once again very good correlation is achieved with the finite element solutions and the finite difference solutions of Mehryan *et. al*. [54]. Confidence in the present finite element code is therefore justifiably high. In the second validation, we implement a different computational technique to solve the entire general boundary value problem as defined by Eqns. (10)-(13) under boundary conditions (15). The fundamental premise of generalized differential quadrature (GDQ) is that the derivative of a function with respect to a space variable on a given set of points is approximated as a weighted

linear sum at the selected points in the domain of that variable. The GDQ approach was pioneered in fluid mechanics and engineering dynamics applications by Shu *et al.* [61] to improve the Bellman differential quadrature (DQM) method developed in the early 1970s. It approximates the spatial derivative of a function with respect to a space coordinate at a given grid point as a weighted linear sum of all the functional values at all grid points in the whole domain of that space coordinate. The computation of weighting coefficients by GDQ is based on the analysis of a high order polynomial approximation and the analysis of a linear vector space. The weighting coefficients of the first order derivative are calculated by a simple algebraic formulation, and the weighting coefficients of the second and higher order derivatives are given by a recurrence relationship. It has been shown by Shu *et al.* [61] that the GDQ approach is equivalent to the *highest order finite difference scheme*. This method is also described in some detail in the context of magnetohydrodynamics by Bég [68]. To illustrate the approximation in the GDQ, let us consider a function $f(\eta)$ defined in the domain $0 < \eta \leq a$. According to the GDQ, the function $f(\eta)$ can be approximated as follows:

$$\left.\frac{\partial^r f(\eta)}{\partial \eta^r}\right|_{\eta,\tau=\eta_i} = \sum_{m=1}^{N_\eta} A_{im}^{(r)} f(\eta_m) = \sum_{m=1}^{N_\eta} A_{ij}^{(r)} f_m\,, \quad i = 1, 2, \ldots, N_\eta. \tag{25}$$

Therefore, the weighting coefficients for the first-order derivatives in the η_i direction are given by the formula [61, 68].

$$A_{ij} = \begin{cases} -\sum_{j=1,\ i\neq j}^{N_\eta} A_{ij}, & i = j, \\ \frac{1}{a}\frac{M(\eta_i)}{(\eta_i - \eta_j)M(\eta_j)}, & i \neq j, \end{cases} \qquad i, j = 1, 2, \ldots, N_\eta, \qquad M(\eta_i) = \prod_{j=1,\ i\neq j}^{N_\eta} (\eta_i - \eta_j) \tag{26}$$

The weighting coefficients of the higher-order derivative can be obtained as follows [61, 68]:

$$\left[A_{ij}^{(r)}\right] = \left[A_{ij}^{(r-1)}\right][A_{ij}] = [A_{ij}]\left[A_{ij}^{(r-1)}\right]. \tag{27}$$

It is pertinent to deploy Chebyshev-Gauss-Lobatto grid distribution:

$$\frac{\eta_i}{a} = \frac{1}{2}\left[1 - \cos\left(\frac{i-1}{N_\eta - 1}\pi\right)\right] \qquad i = 1, 2, \ldots, N_\eta, \tag{28}$$

According to the GDQ, the discretized governing equations and the appropriate boundary conditions can then be generated, although for brevity we have omitted these lengthy algebraic expressions here. In the emerging formulations, parameters *B* and *C* arise, which represent the *second- and third-order weighting coefficients*, respectively. The values of the similarity flow variables i.e. f_i, θ_i , φ_i and $\chi_i$at each node in the solution domain can be obtained. These may then in turn be utilized to compute the wall functions i.e. reduced skin friction, Nusselt number, Sherwood number and motile micro-organism wall mass flux. Comparisons of the finite element code and the GDQ code (which is executed on an SGI Octane desk workstation and takes forty seconds to converge) for skin friction coefficient , $\sqrt{\frac{n+1}{2}}f''(0)$, and Sherwood number, $\sqrt{\frac{n+1}{2}}\emptyset'(0)$ are presented in Tables 3 and 4 respectively, with all parameter data given. There is very good correlation between both methods for reduced skin friction coefficient ($\sqrt{\frac{n+1}{2}}f''(0)$) at all values of thermophoresis nanoscale parameter (*Nt*) and buoyancy ratio parameter (*Nr*) (in Table 3) and also for reduced Sherwood number ($\sqrt{\frac{n+1}{2}}\emptyset'(0)$) at all simulation values of thermophoresis nanoscale parameter (*Nt*) and Brownian motion nanoscale parameter (*Nb*) (in Table 4). Confidence in the present FEM code is therefore again very high. Furthermore Tables 3 and 4 provide a solid benchmark for other researchers to extend the current model and to compare alternative numerical methods with the present FEM and GDQ techniques.

Table 2: Comparison of results for the density gradient of motile micro-organisms $\sqrt{\frac{n+1}{2}}\chi'(0)$for *n = 1, M = Nb = 1, Ec = 0, Nr = Nt = Gr = 0.5, Lb = Le = 2, Rb = 0.3, δ = 0°, b (chemotaxis constant) =1,* and different values for micro-organism concentration difference parameter (*Ω*) and biconvection Péclet number (*Pe*).

	Pe = 0.3		**Pe = 0.5**		**Pe = 0.5**	
Ω	Present code	Mehryan *et. al* [54]	Present code	Mehryan *et. al* [54]	Present Code	Mehryan *et. al* [54]
0.1	2.80479	2.819	3.20986	3.203	3.59853	3.598
0.2	2.84746	2.861	3.28579	3.275	3.70988	3.699
0.4	2.93298	2.945	3.43801	3.418	3.903	3.93266

0.6	3.01871	3.029	3.55134	3.561	4.15565	4.107
0.8	3.10416	3.114	3.70218	3.704	4.30139	4.311
1.0	3.18983	3.197	3.85296	3.847	4.515	4.52098

Table 3: Results for skin friction coefficient , $\sqrt{\frac{n+1}{2}}f''(0)$, with *Gr = n = Pe = M = Lb = 1, Ec = Rb = Ω = Nb = 0.1, Pr = 10, δ = 0°* and different values for *Nt* and *Nr* with finite element method (FEM) and Generalized Differential Quadrature (GDQ).

	FEM	**GDQ**	**FEM**	**GDQ**	**FEM**	**GDQ**
Nr	*Nt = 0.05*		*Nt = 0.1*		*Nt = 0.5*	
0.3	1.22202	1.22301	1.22392	1.22407	1.224	1.22439
0.5	1.28574	1.28614	1.2979	1.2964	1.3075	1.30721
0.8	1.38412	1.38516	1.41402	1.41509	1.44224	1.44274
0.4	1.45193	1.45204	1.49629	1.49598	1.54296	1.54288
0.5	1.52195	1.52178	1.58451	1.58397	1.66415	1.66409

Table 4: Results for Sherwood number, $\sqrt{\frac{n+1}{2}}\emptyset'(0)$, with *Le = Pe = 10, n = 1, δ = 0°, M =Ec = Nr = Rb = Pe = Lb = Ω = 0,* and different values for *Nt* and *Nb* with finite element method (FEM) and Generalized Differential Quadrature (GDQ).

	FEM	**GDQ**	**FEM**	**GDQ**	**FEM**	**GDQ**
Nb	*Nt = 0.1*		*Nt = 0.3*		*Nt = 0.5*	
0.1	2.11927	2.11934	2.40624	2.40636	2.363477	2.363428
0.2	2.27421	2.27442	2.48186	2.48171	2.43115	2.431221
0.1	2.52916	2.52941	2.57045	2.57067	2.48106	2.481142
0.1	2.78961	2.78955	2.64549	2.64503	2.5212	2.523413
0.1	3.04169	3.04158	2.70776	2.70794	2.56326	2.563744

Table 1 shows that reduced Nusselt decreases with increase in Brownian motion parameter (*Nb*) and thermophoresis parameter (*Nt*). The erratic motions of nanoparticles in fluid give rise to an increase in temperature (transfer of heat to the boundary layer from the wall) and hence heat transfer rates at the wall (sheet) decrease. From **Table 2** it is evident that an increase in the motile micro-organism wall flux (density gradient at the sheet surface) accompanies an increment in micro-organisms concentration difference parameter (**Ω**) and bioconvection Péclet number (*Pe*) since both these parameters deplete the concentration of motile micro-organisms within the boundary layer, as will be elucidated later. **Table 3** shows that the local skin friction coefficient increases with increase in buoyancy ratio parameter (*Nr*) and thermophoresis parameter (*Nt*). **Table 4** shows that Sherwood number i.e. dimensionless wall nano-particle mass transfer rate increases with increasing Brownian motion parameter (*Nb*) and thermophoresis parameter (*Nt*).

5. FINITE ELEMENT METHOD NUMERICAL RESULTS AND DISCUSSION

Figs 2-10 illustrate the FEM results graphically for variation in selected parameters, namely *sheet inclination angle (δ), Brownian motion parameter (Nb), thermophoresis parameter (Nt), Richardson number i.e. Ri= Gr/Re^2) buoyancy ratio parameter (Nr), Eckert number (Ec), bioconvection Rayleigh number (Rb), Lewis number (Le), bioconvection Lewis number (Lb), bioconvection Peclet number (Pe), micro-organism concentration difference parameter (Ω). The plots illustrate the evolution in the primitive similarity flow characteristic variables, velocity field f′(η), temperature profile θ(η), nanoparticle concentration φ(η)* and *density of gyrotactic micro-organisms χ(η).* Careful selection of data has been conducted based on actual industrial recommendations and robust simulations.

5.1 Velocity Variation

The effect of various thermophysical parameters on velocity profiles are depicted in **Figs. 2a-c.** It can be seen from Fig 2(a) that velocity decreases with an increase in the angle of inclination of the stretching sheet (δ) increases.

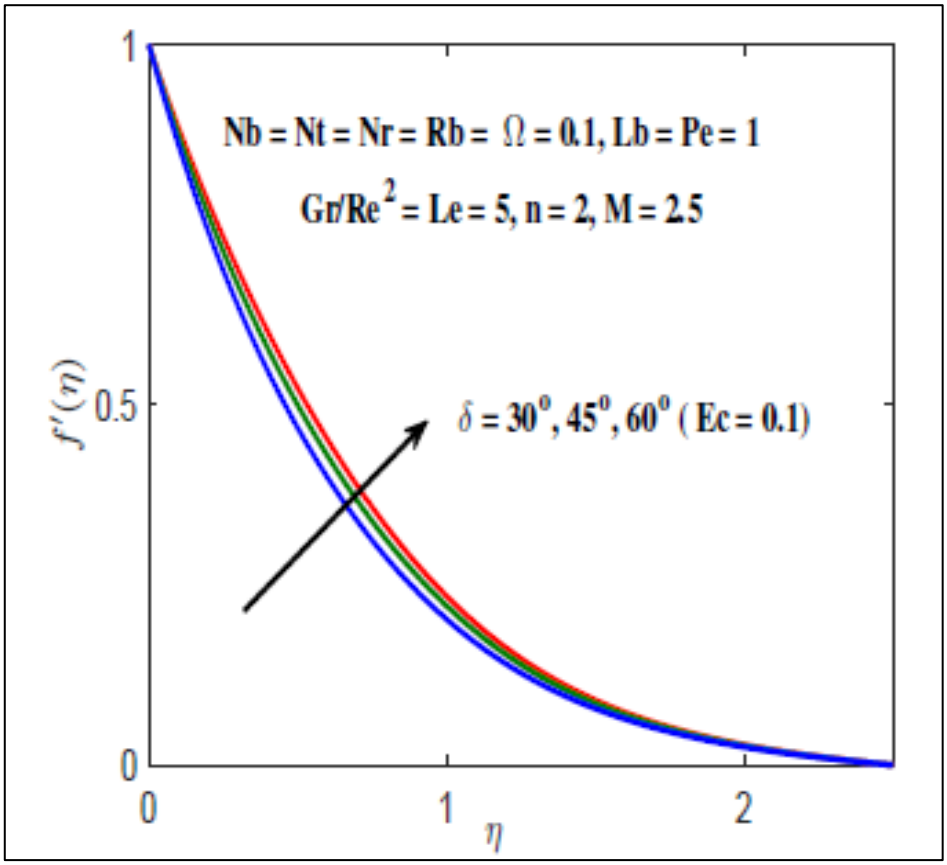

(a) Effect of angle of inclination of sheet (δ)

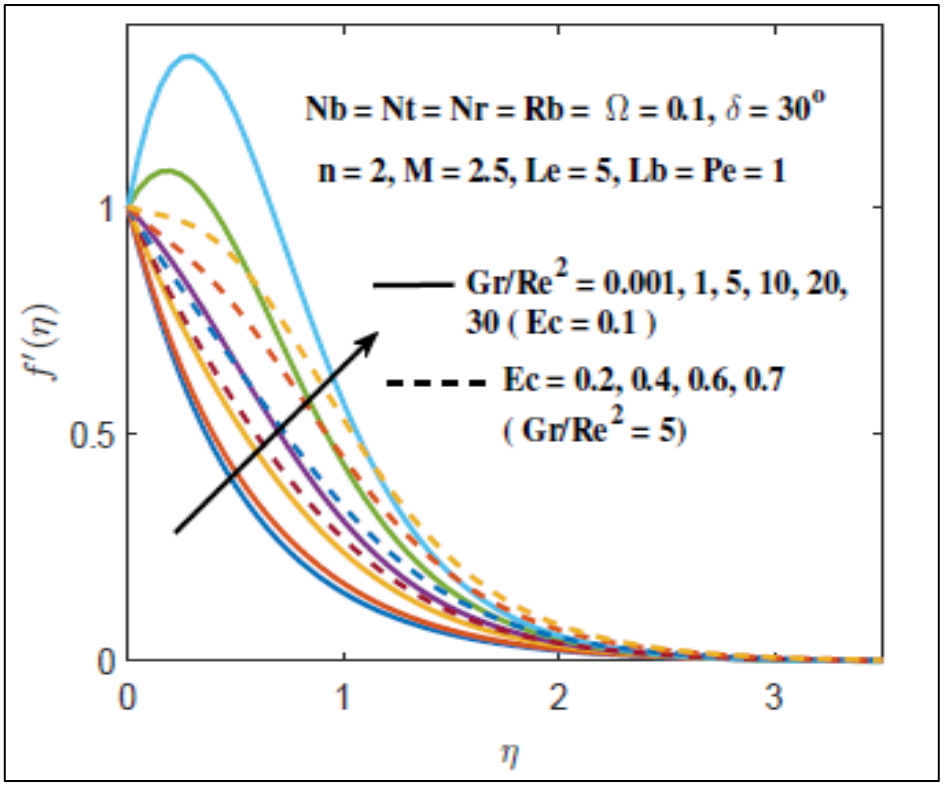

(b) Effect of Eckert number (*Ec*) and Richardson number (*Ri* = *Gr/Re*^{2})

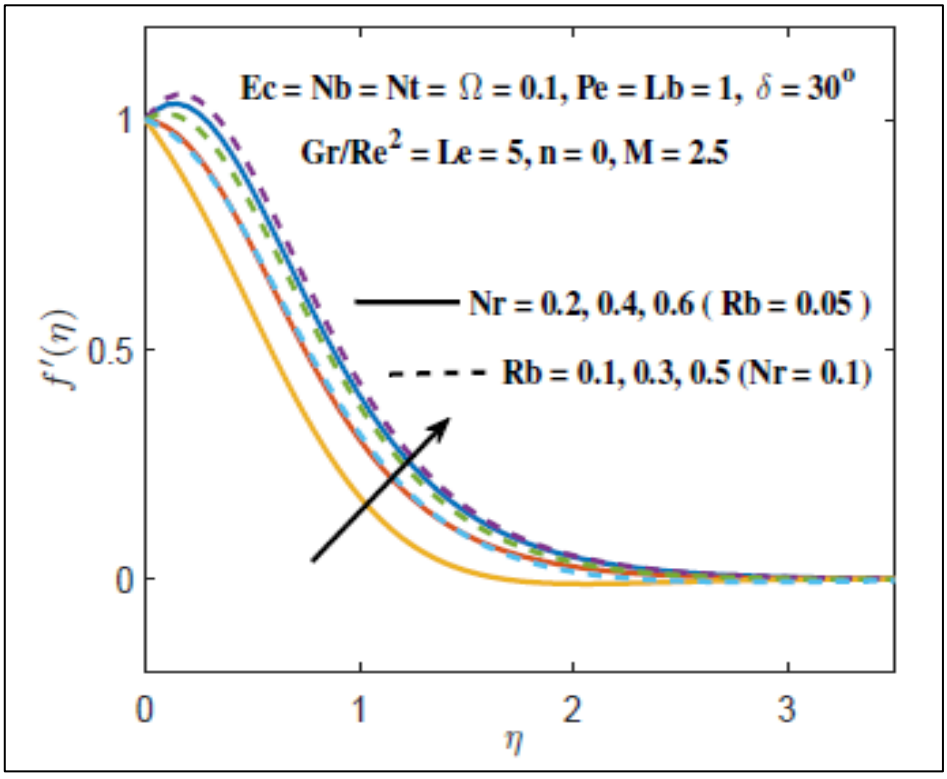

(b) Effect of buoyancy ratio (*Nr*) and bioconvection Rayleigh number (*Rb*)

Figures 2a, b, c: Effects of various thermophysical parameters on *velocity* profiles

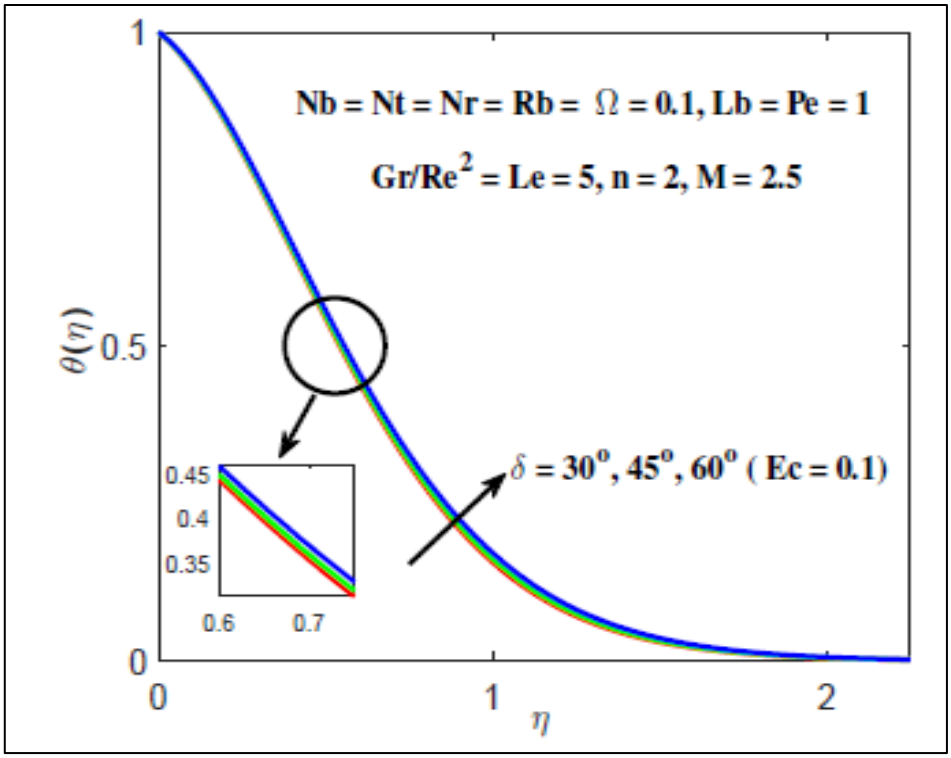

(a) Effect of angle of inclination of sheet (δ)

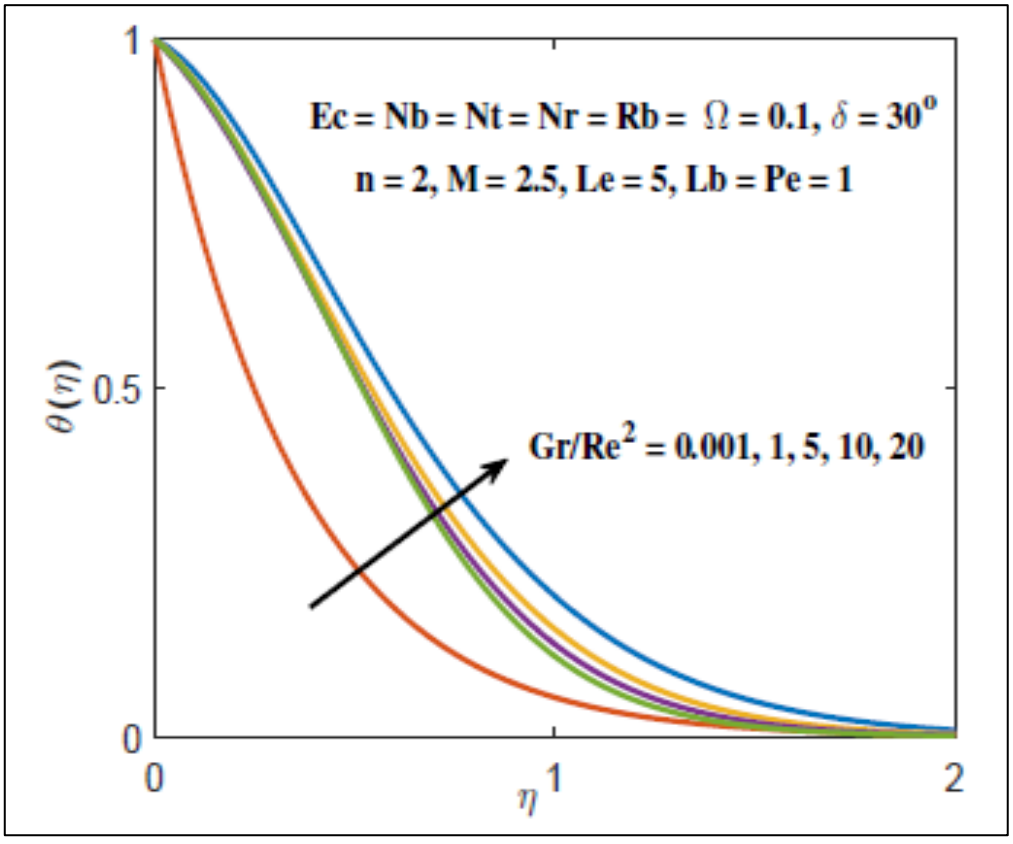

(b) Effect of Richardson number ($Ri = Gr/Re^2$)

Figures 3a, b: Effects of various thermophysical parameters on *temperature* profiles

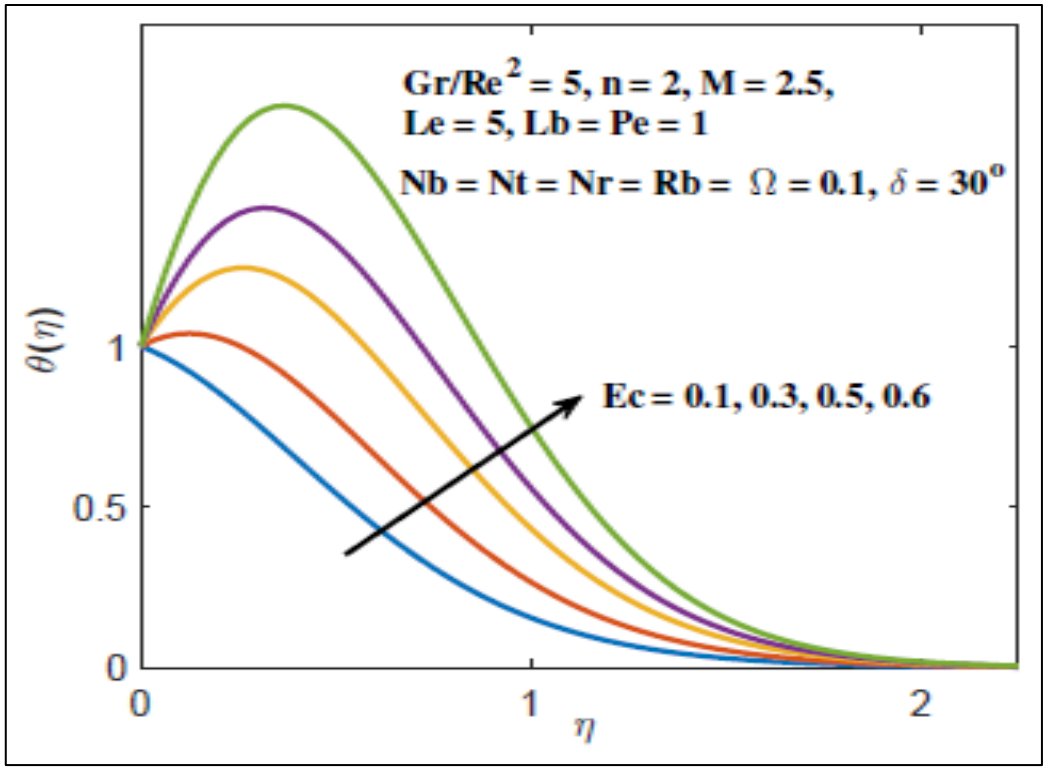

(a) Effect of Eckert number (*Ec*)

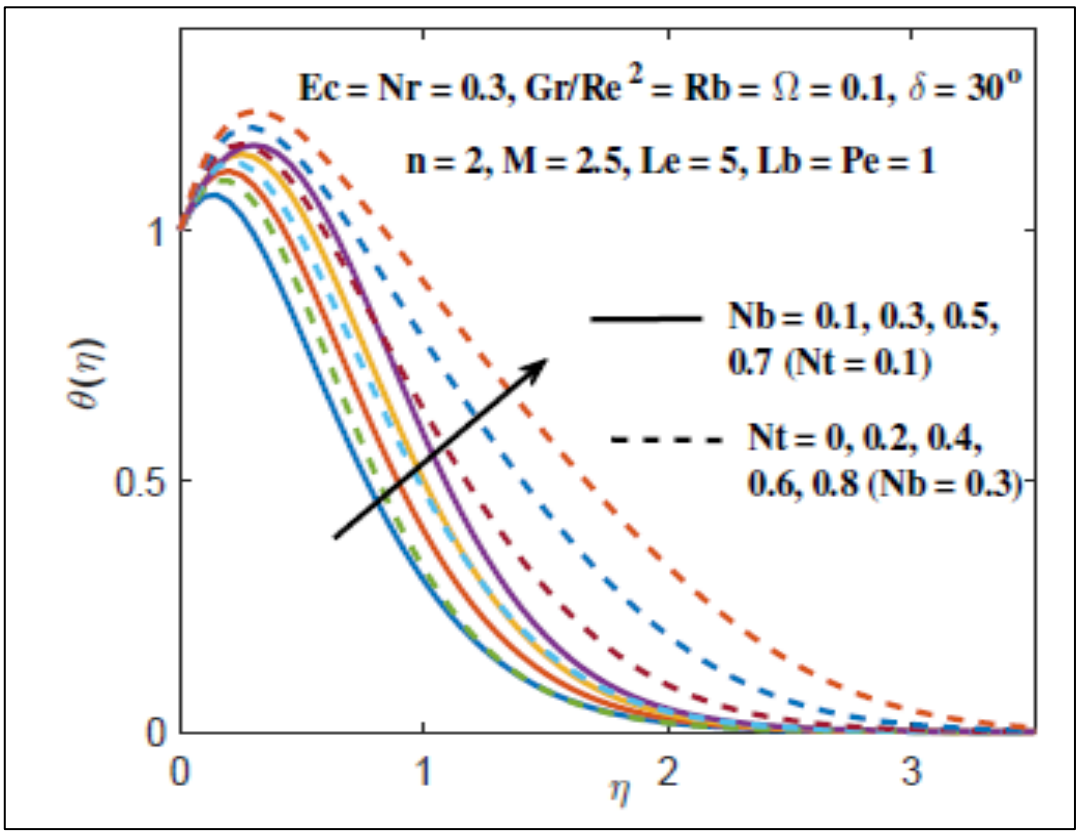

(b) Effect of nanoscale Brownian motion parameter (*Nb*) and thermophoresis parameter (*Nt*)

Figures 4a, b: Effects of various thermophysical parameters on *temperature* profiles

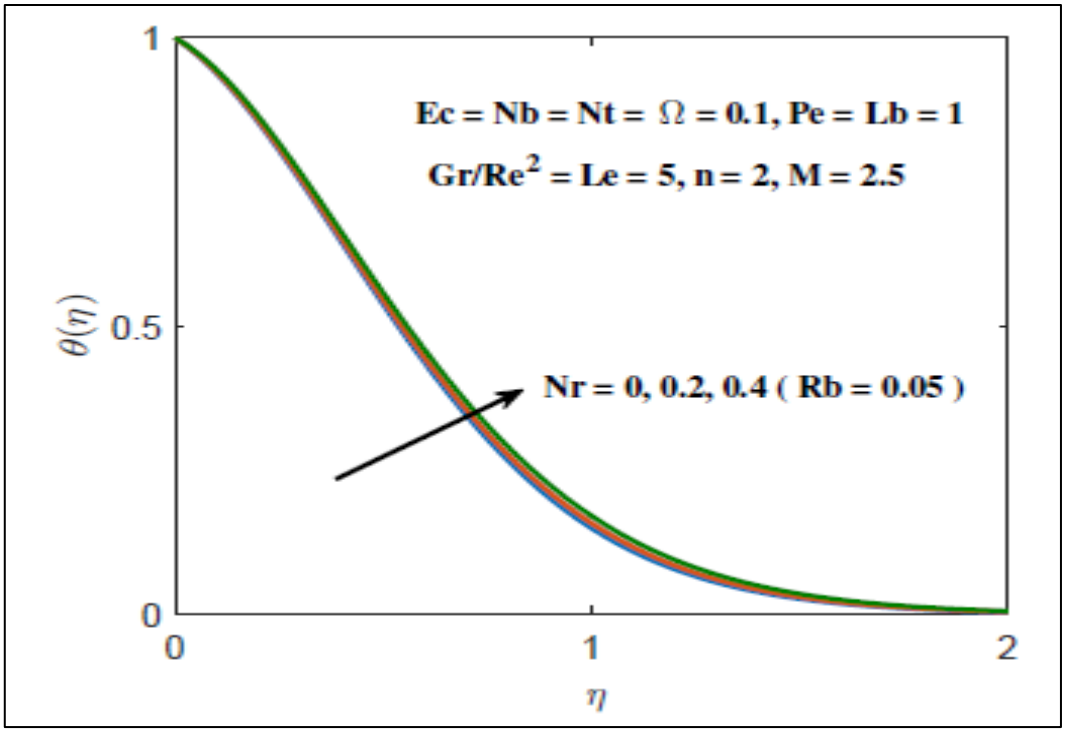

Figure 5: Effect of buoyancy ratio parameter (*Nr*) on *temperature* profiles

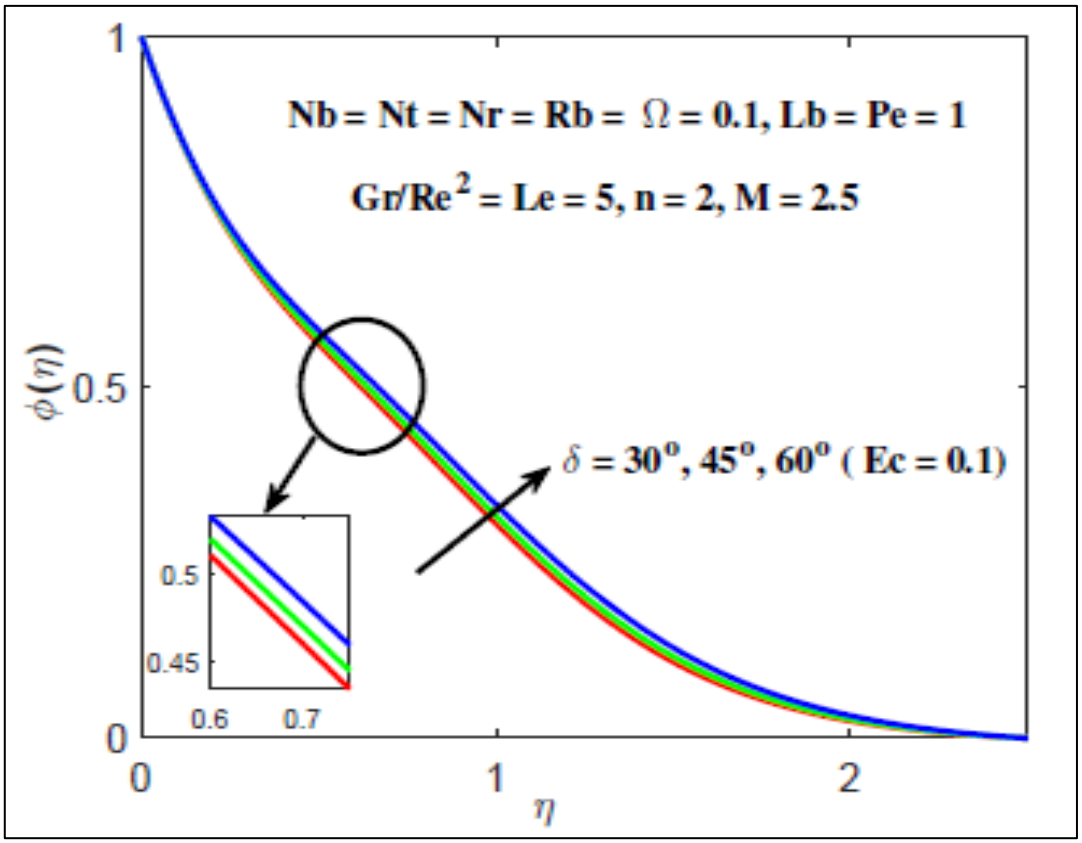

(a) Effect of angle of inclination of sheet (*δ*)

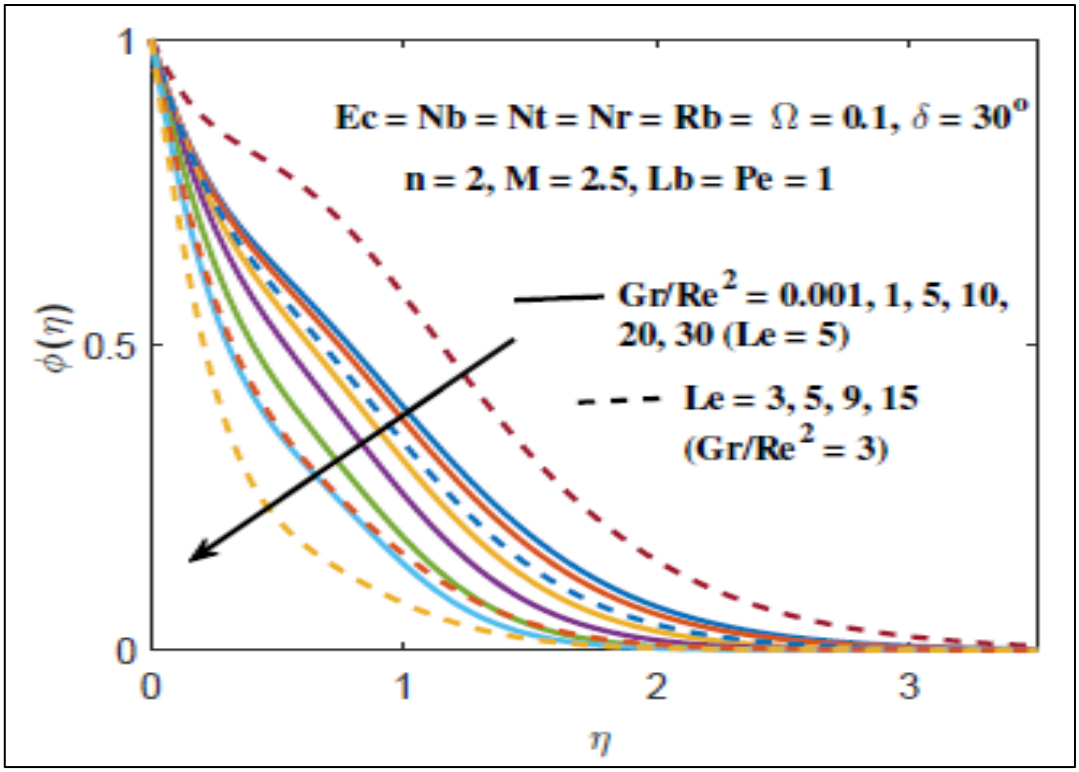

(b) Effect of Richardson number (*Ri* = *Gr/Re*^{2}) and Lewis number (*Le*)

Figures 6a, b: Effects of various thermophysical parameters on *nanoparticle concentration*

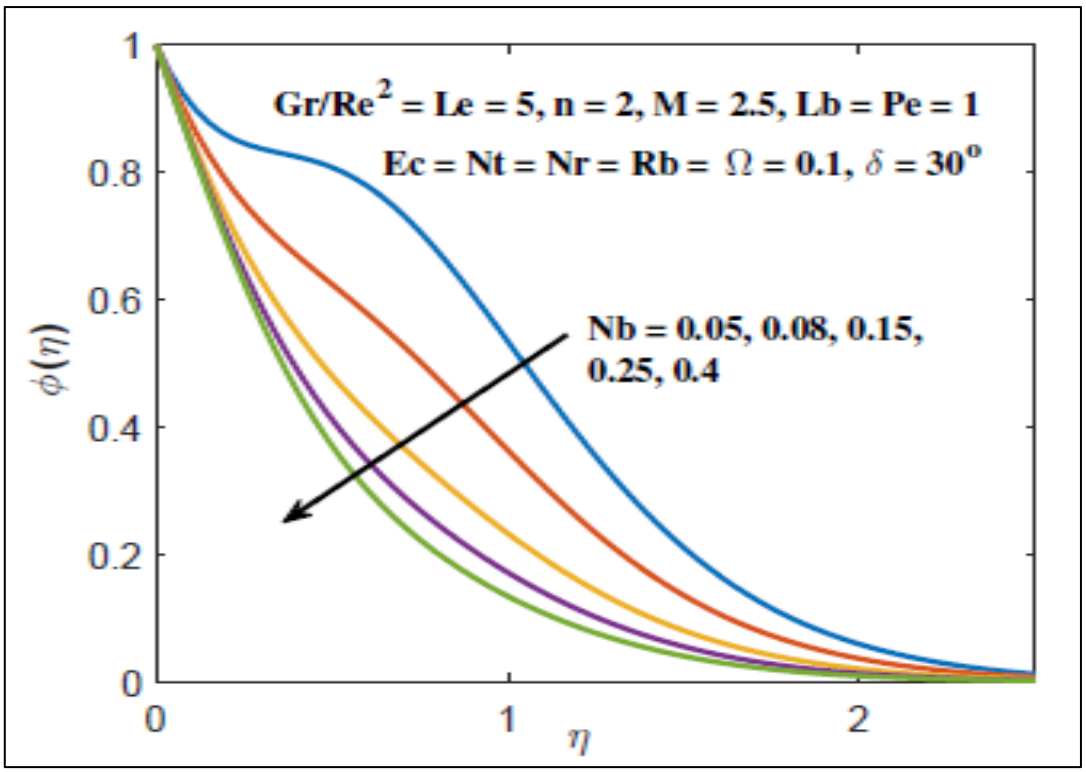

(a) Effect of nanoscale Brownian motion parameter (*Nb*)

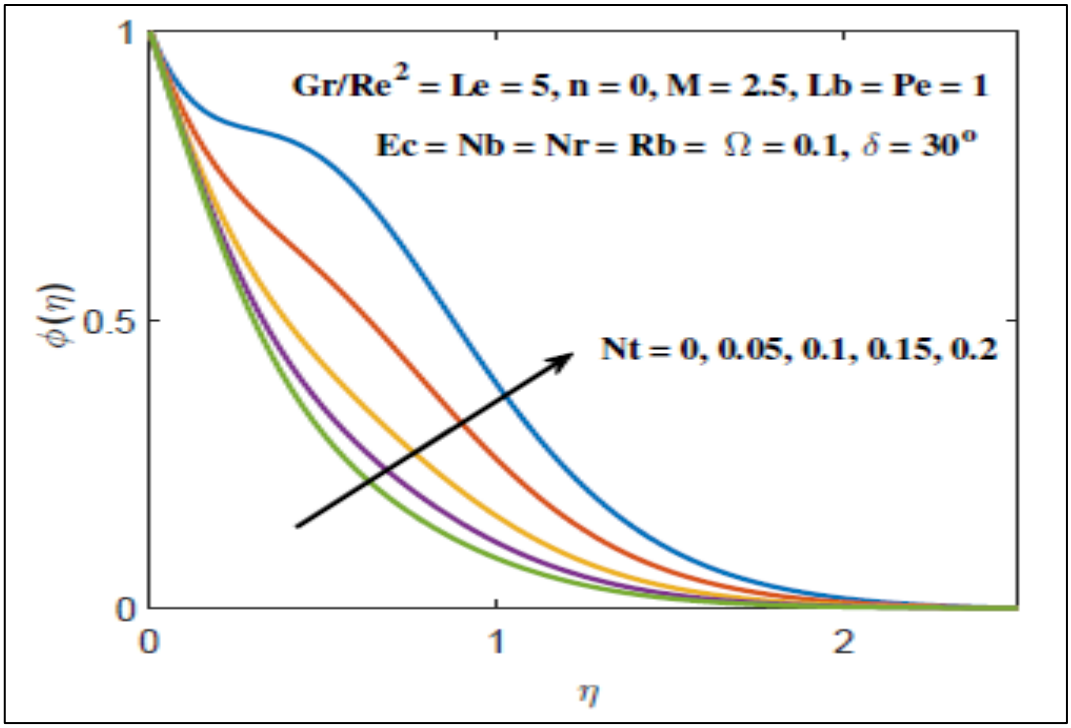

(b) Effect of nanoscale thermophoresis parameter (*Nt*)

Figures 7a, b: Effect of various thermophysical parameters on *nanoparticle concentration*

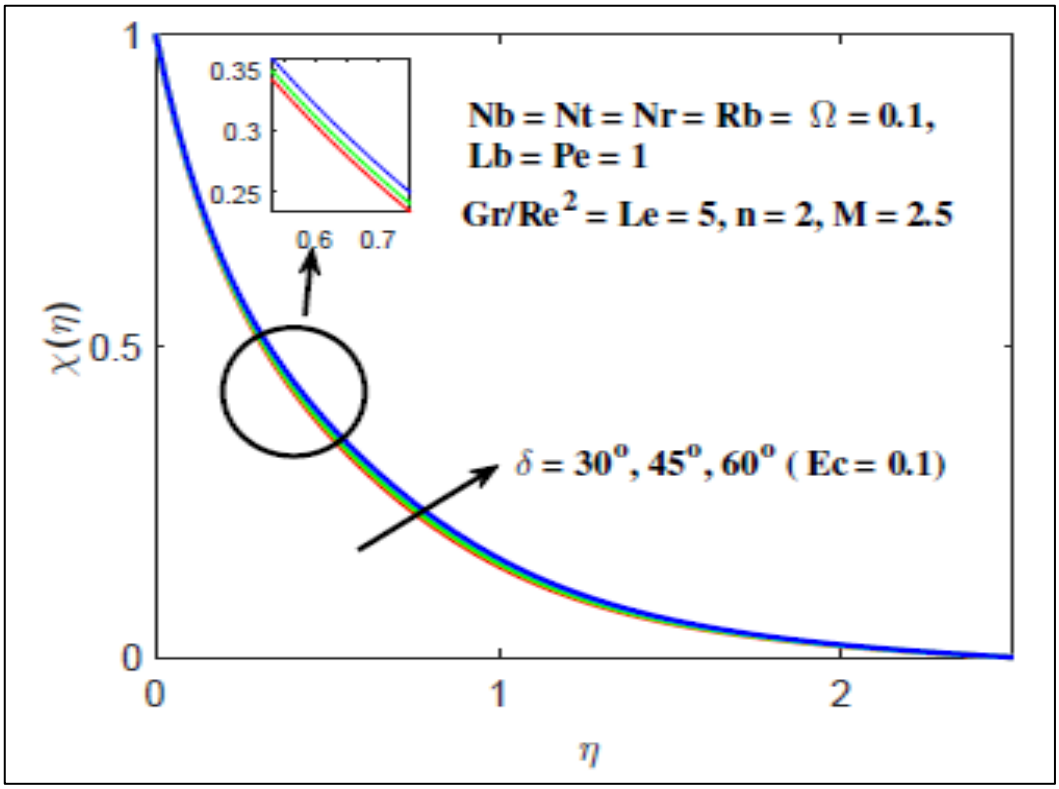

(a) Effect of angle of inclination of sheet (*δ*)

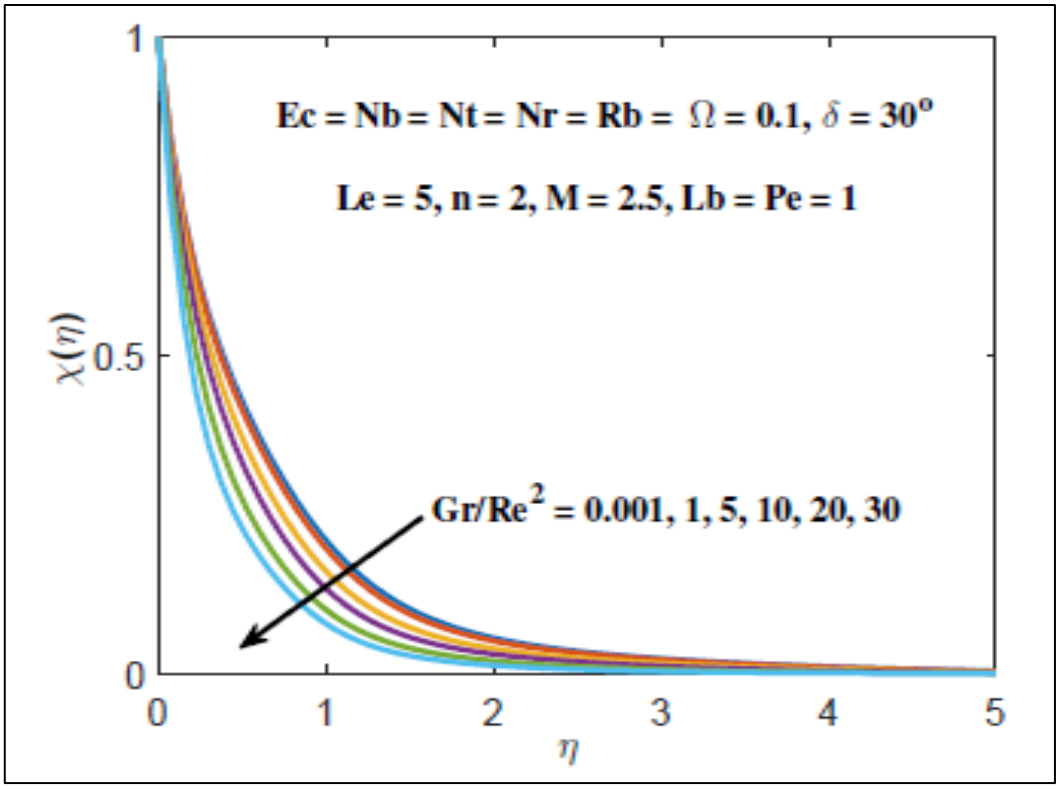

(b) Effect of Richardson number (*Ri* = *Gr*/*Re*^{2})

Figures 8a, b: Effects of various thermophysical parameters on *motile micro-organism density number*

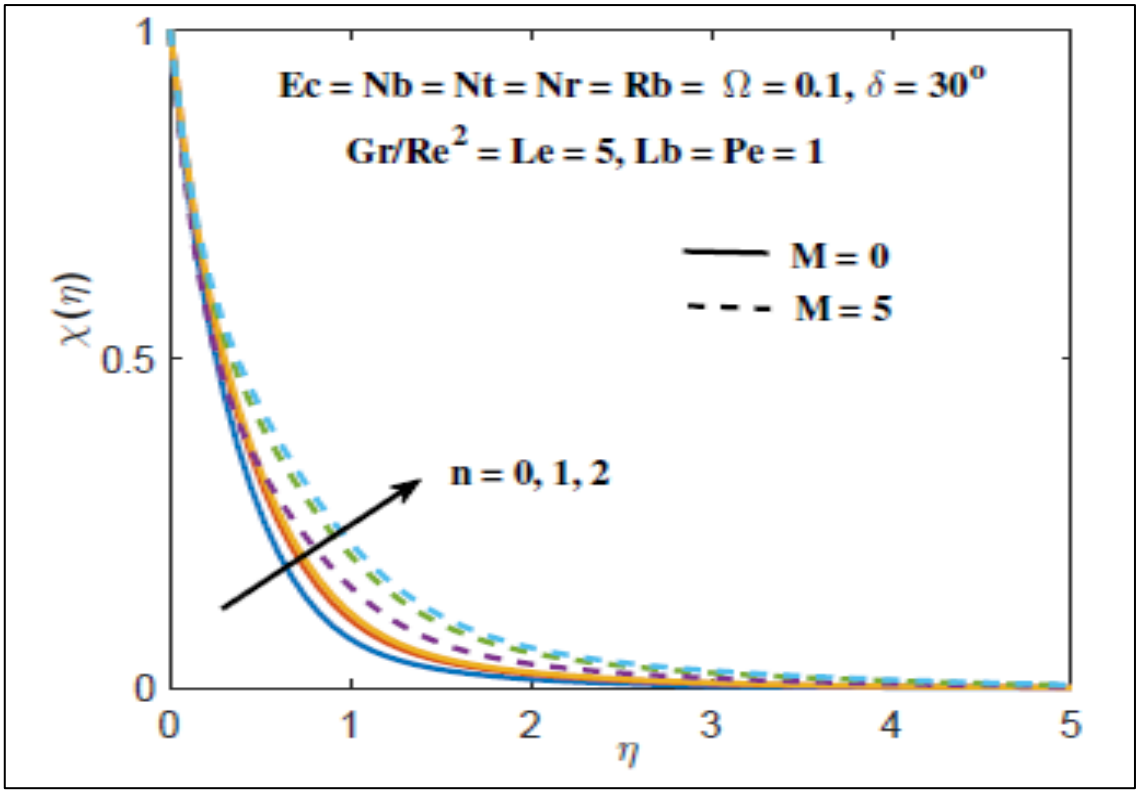

(a) Effect of magnetic body force parameter (*M*) and nonlinear stretching parameter (*n*)

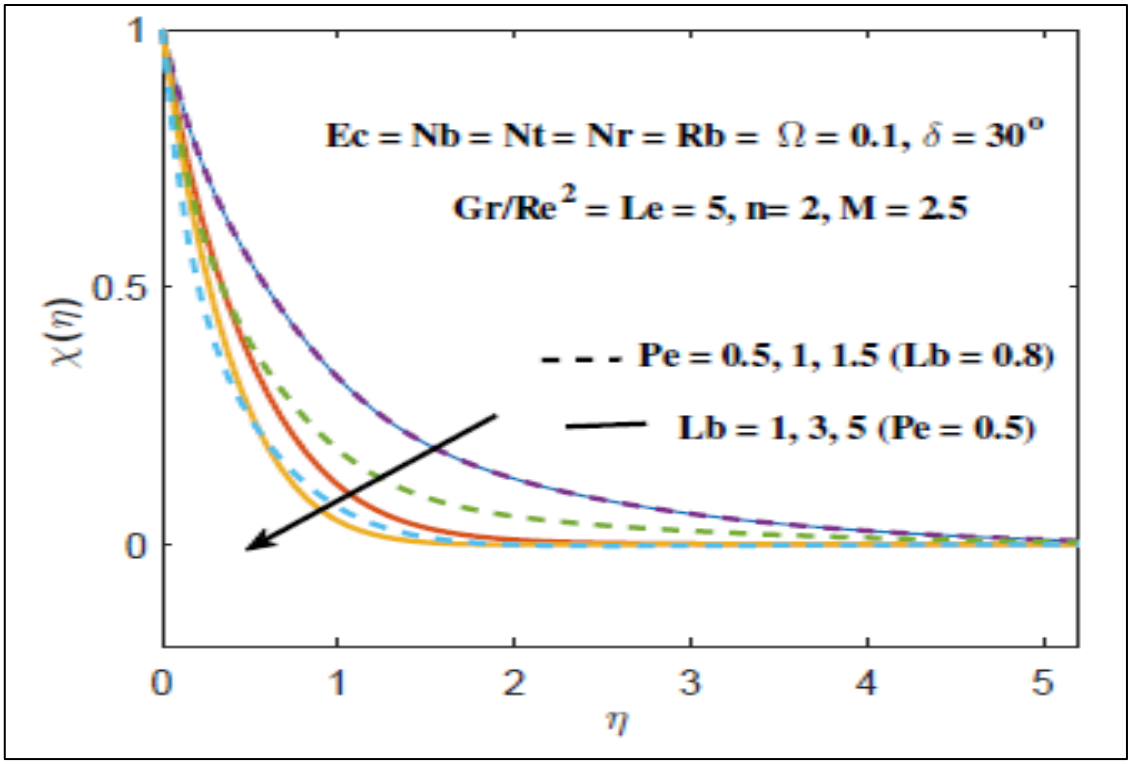

(b) Effect of bioconvection Lewis number (*Le*) and bioconvection Péclet number (*Pe*)

Figures 9a, b: Effects of various thermophysical parameters on *motile micro-organism density number*

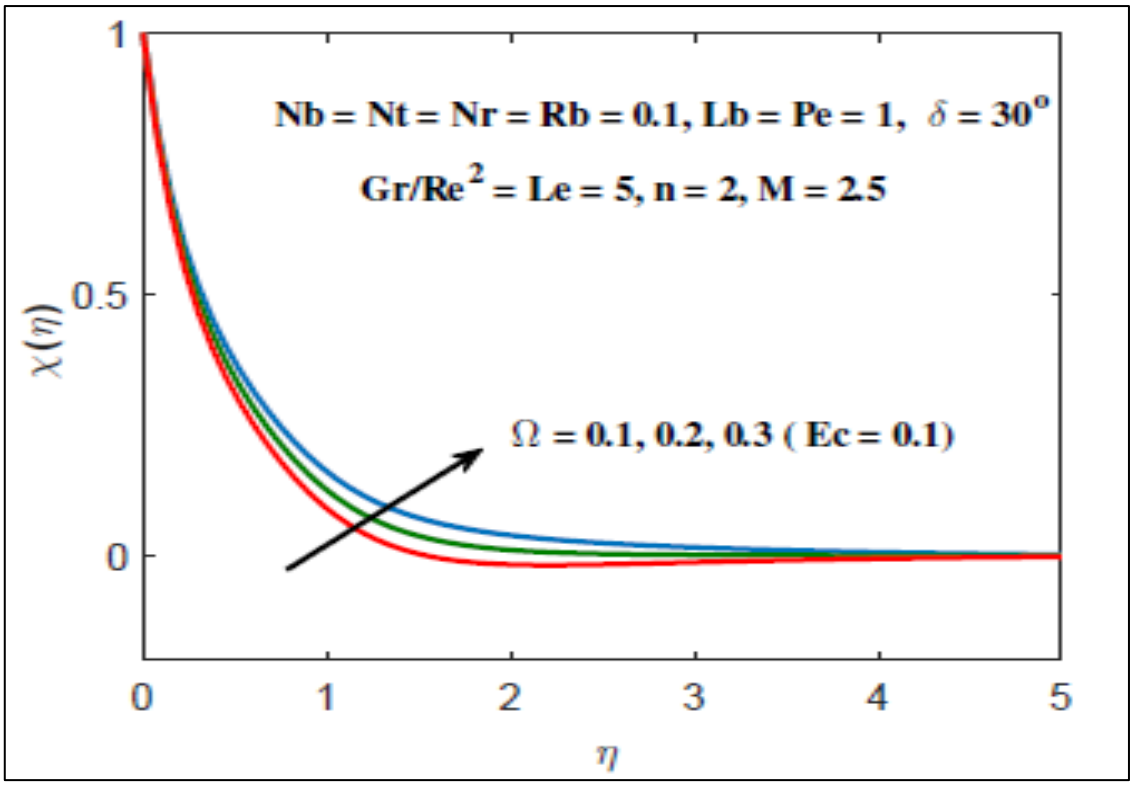

Figure 10: Effect of micro-organism concentration difference parameter (*Ω*) on *motile micro-organism density number*

This is due to the fact that with increasing angle of inclination (δ) the buoyancy forces are increased. Since only the *thermal buoyancy force*, $\left(\frac{2}{n+1}\right)\left(\frac{Gr}{Re^2}\right)(\theta cos\delta)$, in Eqn (10), is *positive* it follows that greater inclination angle will assist momentum development. However, the contributions from the nano-particle species buoyancy and motile micro-organism species buoyancy forces i.e. the terms, $\left(\frac{2}{n+1}\right)\left(\frac{Gr}{Re^2}\right)(-Nrcos\delta - Rb\chi cos\delta)$, are *negative*. They increasingly oppose momentum development, leading to flow deceleration. These negative buoyancy forces are however dominated by the stronger thermal buoyancy force (since very *small Nr and Rb* values are simulated) and therefore the *net effect is flow acceleration*, as observed in Fig. 2a. Overall therefore there will occur a decrease in momentum (hydrodynamic) boundary layer thickness in the coating flow regime. The impact of Richardson number (Ri = Gr/Re^2) and Eckert number (Ec) on velocity evolution is depicted in Fig 2(b). Generally natural convection is negligible when $Ri < 0.1$ whereas forced convection is negligible when $Ri > 10$. Both forced and free convection contribute when $0.1 < Ri < 10$. It may be noted that invariably forced convection is large relative to natural convection except in the case of extremely low forced flow velocities. As the Richardson number increases, there is a substantial elevation in flow velocity accompanying an accentuation in natural convection which becomes dominant. For high Ri values (>10) the monotonic decay of profiles morphs and a velocity overshoot is observed near the sheet surface. This overshoot is enhanced and displaced further from the sheet surface as Ri increases from 20 to 30. Marked reduction in hydrodynamic boundary layer thickness is therefore induced with greater Richardson number (stronger natural convection buoyancy effect) as a result of the strong flow acceleration. It is also seen in Fig 2(b) that velocity also increases with an increase in Eckert number, in particular near the wall. The Eckert number expresses the relative contribution of kinetic energy in the flow and the enthalpy difference in the boundary layer. At very low values of Ec embodies the conversion of kinetic energy into thermal energy by work done against the viscous fluid stresses, as elaborated by Gebhart [55]. However, at higher values this dissipation effect can accelerate incompressible flows, especially when Ohmic dissipation is present in the energy equation, as observed in Fig. 2b, in particular, when it is combined with the *momentum imparted via nonlinear stretching* of the sheet. This effect has also been observed in nanofluids by Ibrahim [16] and more recently by Thumma *et al.* [17]. Viscous fluid stresses have been shown to respond differently to dissipation effects (which occur at the molecular level) in nanofluid dynamics when purely magnetic Lorentz force is only present and when there is the additional effect of Ohmic dissipation (Joule heating). Positive Eckert number (as studied here)

implies cooling of the wall and therefore a transfer of heat to the magnetized nanofluid. The presence of a strong magnetic field (M= 2.5 i.e. magnetic Lorentz force is 250% greater than the viscous hydrodynamic force) may also contribute to dissipation effects, as noted by Ibrahim and Shankar [10]. However, the unusual response is most likely attributable to the presence of Ohmic dissipation. It is also noteworthy that Prandtl number (Pr) is prescribed unity value which is appropriate for highly-doped water-based nanofluid suspensions. The no-slip condition enforced in the wall boundary conditions in Eqn. (15) requires that the flow velocity at the surface of a solid object (i.e. sheet surface) is zero and that the fluid temperature is equal to the surface temperature. The thermal boundary layer thickness is similarly the distance from the body at which the temperature is 99% of the temperature found from an inviscid solution. The ratio of the two thicknesses is dictated by the Prandtl number. For Prandtl number of unity, both the hydrodynamic and thermal boundary layers are of the same thickness. However, when Prandtl number exceeds unity, the thermal boundary layer is thinner than the velocity boundary layer. Generally, higher Pr fluids will have relatively low thermal conductivities which will suppress thermal conduction heat transfer *from the wall* and reduce thermal boundary layer thickness, resulting in lower nanofluid temperatures in the boundary layer regime which is undesirable in solar coating nano-materials. Smaller values of Pr are equivalent to increasing thermal conductivities, and therefore heat is able to diffuse away from the heated plate more rapidly than for higher values of Pr and a nominal value of $Pr = 1$ is appropriate for solar aqueous nano-material coatings. Evidently from Fig 2(c) the velocity profile is enhanced with greater values of bioconvection Rayleigh number Rb. The classical Rayleigh number embodies the ratio of buoyancy and viscosity forces multiplied by the ratio of momentum and thermal diffusivities. The bioconvection Rayleigh number however is a modified form of the classical Rayleigh number and instead features a numerator which is representative of the buoyancy contribution from motile microorganism species concentration, with a denominator which is associated with thermal buoyancy force. The dominant effect of increasing Rb is to accelerate the magnetic nanofluid boundary layer for some distance away from the plate and to effectively reduce the momentum (velocity) boundary layer thickness. All velocity profiles are observed to converge in the free stream testifying to the imposition of an adequately large infinity boundary condition in the finite element code. In many theoretical studies of bioconvection, the bioconvection Rayleigh number can also be employed to study the hydrodynamic stability of the flow and allows the determination of a critical zone within which bioconvection patterns are generated for a given concentration of motile micro-organisms, although this aspect is beyond the focus of the present work. Fig 2(c) also shows that flow velocity is elevated with

an increase in the buoyancy ratio parameter, *Nr*. *Nr* embodies the relative contribution of nano-particle species buoyancy to thermal buoyancy. When Nr equals unity both contributions are the same. However, for *Nr* <1 (as studied here), the thermal buoyancy dominates the nano-particle species buoyancy and this manifests in acceleration of the boundary layer flow and a decrease in momentum (hydrodynamic) boundary layer thickness. With high values of bioconvection Rayleigh and also buoyancy ratio numbers there is a distinct velocity overshoot in close proximity to the wall. This feature is absent at lower values of these parameters.

Figs. (3-5) illustrate the computed temperature profiles for various thermophysical parameters. In Fig 3(a), it is apparent that at fixed value of other parameters, the temperature (and also thermal boundary layer thickness) increases with increasing angle of sheet inclination, δ. This is again attributable to the greater overall increase in buoyancy (thermal buoyancy component dominating the nano-particle and micro-organism species buoyancy forces) with increasing inclination of the sheet. Moreover, it is observed in Fig 3(b) that dimensionless temperature increases with higher values of Richardson number ($Ri = Gr/Re^2$). Consequently, the thermal boundary layer thickness also is enhanced with an increase in Richardson number. Fig 4(a) demonstrates that temperature of the magnetic nanofluid strongly increases with a rise in Eckert number *Ec*. Greater mechanical energy is converted via internal friction to thermal energy i.e. heat dissipation for higher values of *Ec*. This heats the boundary layer and boosts thermal boundary layer thickness. The implication is that in mathematical models which neglect viscous heating, temperatures will be under-predicted and inaccurate determinations of heat transfer rates at the stretching wall will be computed. It is therefore important in magnetic nanofluid materials processing to include the viscous dissipation effect. Fig 4(b), it reveals temperatures are boosted with greater Brownian motion (*Nb*) and thermophoresis (*Nb*) numbers. Supplementary heat is generated by the interaction of nanoparticles and the base fluid due to Brownian motion and thermophoresis effects. Consequently, the thermal boundary layer becomes thicker and the effect is so prominent that strong temperature overshoots are observed in the vicinity of the stretching sheet for increasing value of *Nb and Nt.* In the Buongiorno model the parameter *Nb* is inversely proportional to the size of nano-particles (which are assumed spherical and homogenously distributed in the base fluid). With greater *Nb* values smaller nano-particles are present and this intensifies the thermal conduction heat transfer from the particles to the surrounding fluid. This achieves the thermal enhancement which characterizes nanofluids [5]. Again, smooth convergence of profiles is noted in the free stream in both Figs 4a, b confirming that a sufficiently large infinity boundary condition has been

employed in the numerical code. Also, it has been seen in Fig 5 that there is inconsiderable enhancement in temperature with increasing buoyancy ratio parameter *Nr*. The nano-particle diffusion is elevated relative to the thermal diffusion with greater *Nr* which respectively boosts the nano-particles species buoyancy force and depletes the thermal buoyancy force. This results in heating of the fluid and an increase in thermal boundary layer thickness.

Figs. 6 – 7 visualize the distributions of nano-particle concentration for different values of parameters such as Richardson number (Gr/Re^2), Lewis number (*Le*), Brownian motion parameter (*Nb*), thermophoresis parameter (*Nt*) and sheet inclination (δ). There is a weak increase in concentration of nanoparticles observed in Fig 6(a) with increasing angle of inclination (δ). The nano-particle concentration is minimized for the vertical sheet case i.e. when the angle of inclination, $\delta = 0$ since the maximum gravitational force resistance is encountered for this case. As angle of inclination goes on increasing strength of gravitational force decreases. The magnitude of the nano-particle buoyancy force in the momentum Eqn. (10) however increases and this assists the nano-particle species diffusion and thickens the nano-particle concentration boundary layer. In Fig 6(b), it is evident that nanoparticle concentration decreases within the boundary layer with an increase in Richardson number ($Ri = Gr/Re^2$) (largely associated with the concomitant flow acceleration). The nanoparticle concentration boundary layer also decreases with increasing Lewis number (*Le*). This parameter represents the ratio of thermal diffusivity of the nanofluid and species diffusivity of the nano-particles. In the present computations, $Le > 1$ which physically implies that thermal diffusivity of the nanofluid always exceeds the species diffusivity of the nano-particles. The rate of nano-particle diffusion is therefore depleted with greater Lewis number which manifests in a strong depression in nano-particle concentrations throughout the boundary layer regime transverse to the surface of the stretching sheet.

Figs. 7 a, b illustrate the impact of Brownian motion parameter and thermophoresis parameter on nano-particle concentration (volume fraction). Fig 7(a) depicts that the increasing values of Brownian motion parameter (*Nb*) result in a significant suppression in nanoparticle concentration magnitudes. Fig 7(b) shows that greater thermophoresis parameter (*Nt*) however boosts the nano-particle concentration distribution. This implies that greater migration of hot nano-particles in the direction of a decreasing temperature gradient results in a thickening in the nano-particle concentration boundary layer thickness. Conversely greater Brownian motion parameter induces the opposite effect.

Figs. 8-10 present the influence of *bioconvection, geometric, magnetic field and nanofluid parameters* on the density of motile gyrotactic micro-organisms. It is noticed in Fig 8(a) and 8(b) that increasing angle of sheet inclination (δ) and Richardson number ($Ri = Gr/Re^2$) exert a similar effect on the motile micro-organism density distribution as they do on nanoparticle concentration. Increasing angle of inclination enhances the density of motile micro-organisms while increasing Richardson number decreases it. Motile micro-organism species boundary layer thickness is therefore elevated with greater sheet inclination whereas it is depressed with increasing Richardson number. Fig 9(a) reveals that with an increment in magnetic parameter *M*, density of motile microorganisms increases. The destruction of nanofluid momentum and deceleration in the flow with greater Lorentz magnetic drag force (featured in the momentum Eqn. (10)) assists in the propulsion of micro-organisms. The presence of Ohmic dissipation in the term, $Ec[(f'')^2 + 2M(f')^2]$ in the thermal boundary layer equation (11) also encourages micro-organism propulsion since it decelerates the boundary layer flow. Micro-organism density number is minimized for $M = 0$ (electrically non-conducting nanofluid) and maximized for strong magnetic field effect with $M = 5$ (Lorentz magnetic drag is five times the magnitude of hydrodynamic viscous force). Moreover Fig. 9a also shows that with increasing nonlinear stretching parameter *n*, the density of motile micro-organisms is boosted within the boundary layer. This confirms the findings of for example Bég *et al.* [13], Ferdows *et al.* [14] and Chiam [62] for magnetohydrodynamic non-linear stretching sheet boundary layers in both nanofluids and viscous Newtonian fluids. It can be seen from Fig 9(b) that density of motile microorganisms is significantly reduced with increasing bioconvection Lewis number (*Lb*) and Péclet number (*Pe*). In conjunction with the bioconvection Rayleigh number (*Rb*) which was discussed earlier, these two parameters dictate the bioconvection phenomena in the boundary layer. Bioconvection Péclet number relates the rate of advection of micro-organisms driven by the flow to the rate of diffusion of micro-organisms under gyrotaxis. Ordinary Péclet number is customarily associated with convective heat transfer processes and usually defines the heat transport via convection to that via thermal conduction. In biconvection, this parameter when sufficiently high has been shown to dramatically alter patterns of the motile micro-organism flow. The source of bioconvection originates from the *internal energy of the micro-organisms,* as described in considerable detail by Bég [7] and earlier Hill and Pedley [32]. With greater swimming speed (higher bioconvection Péclet number), the micro-organisms propel faster and this *decreases their concentrations*. At lower bioconvection Péclet numbers the reverse effect is induced i.e. motility of the micro-organisms is inhibited and they move slower leading to *higher and significantly more homogenous concentrations,* as observed in Fig. 9b.

Mathematically *Pe* correlates the rate of advection of a flow to its rate of diffusion D_n i.e. the species diffusivity of microorganisms. Clearly since $Pe = bW_c/D_n$, for a given chemotaxis constant, *Pe* is directly proportional to W_c (constant maximum cell swimming speed) and inversely proportional to D_n (the diffusivity of micro-organisms). For $Pe>1$, swimming motions will dominate species diffusivity of micro-organisms and this will lead to a reduction in density of motile micro-organisms. The converse behaviour would arise for $Pe<1$. This parameter can therefore be manipulated via the selection of different micro-organisms to achieve a different distribution in combination with different nano-particles, in for example, the constitution of solar magnetic nano-bio fluid coatings, leading to a change in eventual performance of the coating when deployed on field solar collectors, as noted in [25]-[31]. In fact, bioconvection Péclet number is the ratio of the *characteristic velocity due to gyrotactic swimming* to a *characteristic velocity due to random diffusive swimming*. Since the microorganisms are heavier than water, their up-swimming creates unstable density stratification and an increase in bioconvection Rayleigh number would make the system less stable. The bioconvection Lewis number helps in decreasing the microorganism concentration layer thickness. Physically this is explained by the fact that as the bioconvection Lewis number rises, the *viscous diffusion rate enhances* which in turn decreases the dimensionless velocity and consequently decreases the density of the microorganisms. Bioconvection Lewis number therefore relates the viscous diffusion rate (viscosity of fluid) to the motile micro-organism diffusivity. When this parameter is equal to unity both viscous diffusion and motile micro-organism diffusion rates are the same. The aiding effect of increasing *Lb* is attributable to the decrease in D_n relative to α_m. The motile microorganism rescaled density boundary layer thickness is decreased both with increasing *Lb* and *Pe* numbers. The decrease in density implies a reduction in settling of micro-organisms with greater bioconvection. This encourages mixing and species diffusion in the nanofluid. The introduction of nano-particles into the bioconvection regime also modifies the distributions of motile micro-organisms. There is a significant interaction in both nanofluid and bioconvective mechanisms (both nano-particle and micro-organism species conservation equations are strongly coupled to each other) and careful selection of both can lead to optimized performance of potential magnetic bio-nanofluid aqueous solar coatings. **Fig 10** shows that with increasing values of the micro-organism concentration difference parameter (Ω) there is a *non-trivial enhancement* in the motile micro-organism density number. This parameter arises only in the micro-organism conservation

equation (13) and clearly when increased serves to boost micro-organism concentration boundary layer thickness.

6. CONCLUSIONS

A mathematical model is presented for incompressible, steady-state, boundary layer magneto-bioconvection of a nanofluid (containing motile gyrotactic micro-organisms) over a nonlinear inclined stretching sheet subjected to non-uniform magnetic field, as a simulation of novel bio-nano-material electroconductive solar coatings. The Buongiorno-Kuznetsov nanofluid-bioconvection model is employed and Ohmic dissipation (Joule heating) is incorporated. Via appropriate similarity transformations, the governing partial differential conservation equations are rendered into a system of nonlinear coupled ordinary differential equations subject to physically realistic boundary conditions. A variational finite element method is deployed to solve the emerging non-dimensional boundary value problem. Validation of the general solutions is achieved with a generalized differential quadrature (GDQ) method. Additional validation of several special cases of the model against published results in the literature is also conducted. A detailed parametric study of the impact of bioconvection, magnetic field, geometric (inclination), thermophysical (buoyancy) and nanoscale parameters on key flow characteristics is presented. The main observations of the present study can be summarized as follows:

1)Velocity is decreased (and momentum boundary layer thickness increased) with increasing angle of inclination of the stretching sheet, Richardson number, Eckert number, buoyancy ratio parameter and bioconvection Rayleigh number.

2) Temperature is enhanced (and thermal boundary layer thickness elevated) with increasing angle of inclination, Richardson number, Eckert number, Brownian motion parameter, thermophoresis parameter and buoyancy ratio parameter.

3) Nano-particle concentration (volume fraction) is boosted (and nano-particle concentration boundary layer thickness is also enhanced) with increasing angle of inclination and thermophoresis parameter whereas it is depressed with Richardson number, Lewis number and Brownian motion parameter.

4) Motile micro-organism density number (and therefore also motile micro-organism species boundary layer thickness) is increased with enhancement in angle of inclination, magnetic

parameter and nonlinear stretching parameter whereas it is suppressed with increasing bioconvection Lewis number, bioconvection Péclet number and Richardson number.

5) Local skin friction is increased with greater thermophoresis parameter and buoyancy ratio parameter.

6) Reduced Nusselt number (wall heat transfer rate) is reduced whereas Sherwood number (nano-particle wall species gradient) is enhanced with an increase in Brownian motion and thermophoresis parameters.

7) Motile micro-organism wall density gradient is elevated with an increase in both micro-organism concentration difference parameter and bioconvection Péclet number.

The present study has ignored thermal radiative heat transfer effects which are also important in high-temperature solar engineering and solar nano-materials processing. These will be considered in the future.

ACKNOWLEDGEMENTS

The first author acknowledges the Department of Science and Technology (DST), India for providing financial assistance. The use of Salford University Computational Facilities is also gratefully acknowledged by the last two authors.

REFERENCES

[1] T. Manouras and M. Vamvakaki, Field responsive materials: photo-, electro-, magnetic- and ultrasound-sensitive polymers, *Polym. Chem.*, 8, 74-96 (2017).

[2] A. Paone, M. Joly, R. Sanjines, A. Romanyuk and J.-L. Scartezzini *et al*. Thermochromic films of VO2: W for smart solar energy applications. *SPIE Optics & Photonics Conference, San Diego, California, USA* (2009).

[3] S. Tallósy Preparation and antibacterial properties of reactive surface coatings using solar energy driven photocatalyst, Section: Magnetic Field Assisted Biomaterials Processing, *Handbook of Antimicrobial Coatings*, Pages 89–107, Wiley, New York (2018).

[4] M.J. Uddin, O. Anwar Bég and N.S. Amin, Hydromagnetic transport phenomena from a stretching or shrinking nonlinear nanomaterial sheet with Navier slip and convective heating: a model for bio-nano-materials processing, *J. Magnetism Magnetic Materials*, 368, 252-261(2014).

[5] S. U. S. Choi and J. A. Eastman, Enhancing thermal conductivity of fluids with nanoparticles, developments and applications of non-Newtonian flows, In: *D. A. Siginer and H. P. Wang, Eds., American Society of Mechanical Engineers, New York,* 99-105 (1995).

[6] Das, S. K., Choi, S. U. S., Wenhua, Y., & Pradeep, T., *Nanofluids: Science and Technology,*. New Jersey: Wiley-Interscience, USA (2007).

[7] O. Anwar Bég, Multi-physical computational modelling of nanofluid bioconvection flows in spacecraft bioreactors, *A. Sohail, Z. Li (Eds.): Computational Approaches in Biomedical Nano-Engineering, Wiley-CVH, China,* Chapter 5, pp100-150 (2018). In press

[8] J. Buongiorno, Convective transport in nanofluids, *ASME J. Heat Transfer*, **128**, 240–250 (2006).

[9] R.K. Tiwari, M.K. Das, Heat transfer augmentation in a two-sided lid-driven differentially heated square cavity utilizing nanofluids, *Int. J. Heat Mass Transf.*, **50**, 2002–2018 (2007).

[10] W. Ibrahim and B. Shankar, MHD boundary layer flow and heat transfer of a nanofluid past a permeable stretching sheet with velocity, thermal and solutal slip boundary conditions. *Comput. Fluids,* 75:1–10 (2013).

[11] Puneet Rana, R. Bhargava and O. Anwar Beg, Finite element simulation of unsteady MHD transport phenomena on a stretching sheet in a rotating nanofluid, *Proc. IMECHE- Part N; J. Nanoengineering and Nanosystems,* 227, 77-99 (2013).

[12] P. Rana and O. Anwar Bég, Mixed convection flow along an inclined permeable plate: effect of magnetic field, nanolayer conductivity and nanoparticle diameter, *Applied Nanoscience,* 5, 569-581 (2015).

[13] O. Anwar Bég, M.S. Khan, I. Karim, M.M. Alam and M. Ferdows, Explicit numerical study of unsteady hydromagnetic mixed convective nanofluid flow from an exponentially stretching sheet in porous media, *Applied Nanoscience,* 4 (8) 943-957 (2014).

[14] M Ferdows, MS Khan, O. Anwar Bég, MAK Azad, MM Alam, Numerical study of transient magnetohydrodynamic radiative free convection nanofluid flow from a stretching permeable surface, *Proc. IMechE-Part E: J. Process Mechanical Engineering,* 228 (3) 181-196 (2014).

[15] S. Mansur *et al.,* The magnetohydrodynamic stagnation point flow of a nanofluid over a stretching/shrinking sheet with suction, PLoS One. 10(3): e0117733 (2015).

[16] W. Ibrahim, The effect of induced magnetic field and convective boundary condition on MHD stagnation point flow and heat transfer of nanofluid over a stretching sheet. *IEEE Trans Nanotechnol.,* 14(1):178–186 (2015).

[17] T. Thumma, O. Anwar Bég and A. Kadir, Numerical study of heat source/sink effects on dissipative magnetic nanofluid flow from a non-linear inclined stretching/shrinking sheet, *J. Molecular Liquids,* 232, 159-173 (2017).

[18] T. Hayat *et al.,* Stratified magnetohydrodynamic flow of tangent hyperbolic nanofluid induced by inclined sheet, *Appl. Math. Mech*., 38, 271-288 (2017).

[19] F. T. Zohra, M.J. Uddin and A.I. Ismail, O. Anwar Bég, Bioconvective electromagnetic nanofluid transport from a wedge geometry: simulation of smart electro-conductive bio-nano-polymer processing, *Heat Transfer-Asian Res.* (2017). DOI: 10.1002/htj.21300 (20 pages)

[20] O. Anwar Bég, S. Kuharat, M. Ferdows, M. Das, A. Kadir, M. Shamshuddin, Magnetic nano-polymer flow with magnetic induction and nanoparticle solid volume fraction effects: *solar magnetic nano-polymer fabrication simulation, Computational Thermal Sciences (2018). Under review*

[21] O. Anwar Bég, M. Ferdows, Shamima Islam and M. Nazrul Islam, Numerical simulation of Marangoni magnetohydrodynamic bio-nanofluid convection from a non-isothermal surface with magnetic induction effects: a bio-nanomaterial manufacturing transport model, *J. Mechanics Medicine Biology*, 14, 3, 1450039.1-1450039.32 (32 pages) (2014).

[22] N. A. Órdenes-Aenishanslins, Use of titanium dioxide nanoparticles biosynthesized by *Bacillus mycoides* in quantum dot sensitized solar cells, *Microbial Cell Factories*, 13:90 (2014).

[23] M. Fayaz A, Girilal M, Rahman M, Venkatesan R, Kalaichelvan PT: Biosynthesis of silver and gold nanoparticles using thermophilic bacterium *Geobacillus stearothermophilus*. *Process Biochem*. 46: 1958-1962 (2011).

[24] A. Saxena, Tripathi RM, Zafar F, Singh P: Green synthesis of silver nanoparticles using aqueous solution of *Ficus benghalensis* leaf extract and characterization of their antibacterial activity. *Mater Lett.,* 67: 91-94 (2012).

[25] A.V. Kirthi *et al.,* Biosynthesis of titanium dioxide nanoparticles using bacterium *Bacillus subtilis*. *Mater Lett.*, 65: 2745-2747 (2011).

[26] A.K. Jha, Prasad K, Kulkarni AR: Synthesis of TiO_2nanoparticles using microorganisms. *Colloids Surf B.,* 71:226–229 (2009).

[27] P. Dhandapani, Maruthamuthu S, Rajagopal G: Bio-mediated synthesis of TiO_2nanoparticles and its photocatalytic effect on aquatic biofilm, *J Photochem Photobiol B* 110:43–49 (2012).

[28] T. Klaus-Joerger *et al.,* Bacteria as workers in the living factory: metal-accumulating bacteria and their potential for materials science, *Trends in Biotech*., 19, 15-20 (2001).

[29] K. B. Narayanan and N. Sakthivel, Biological synthesis of metal nanoparticles by microbes, *Advances in Colloid and Interface Science,* 156, 1-13 (2010).

[30] A. Schröfel *et al.,* Applications of biosynthesized metallic nanoparticles – A review, *Acta Biomaterialia,* 10, 4023-4042 (2014).

[31] R. Sadowski et al., Visible light induced photocatalytic inactivation of bacteria by modified titanium dioxide films on organic polymers, *Photochemical & Photobiological Sciences*, 3, 1-10 (2015).

[32] N. Hill, T. Pedley, Bioconvection, *Fluid Dynamics Research* 37, 1-20 (2005).

[33] A. Avramenko, A. Kuznetsov, Stability of a suspension of gyrotactic microorganisms in superimposed fluid and porous layers, *International Communications in Heat and Mass Transfer*, 31 (8) 1057 – 1066 (2004).

[34] T. J. Pedley, N. A. Hill, J. O. Kessler, The growth of bioconvection patterns in a uniform suspension of gyrotactic micro-organisms, *Journal of Fluid Mechanics* 195, 223–237 (1988).

[35] T. J. Pedley and J. O. Kessler, Hydrodynamic phenomena in suspensions of swimming microorganisms, *Ann. Rev. Fluid Mech*., 24, 313-58 (1992).

[36] D. Z. B. J. Y. X. Li H, Liu S, Applications of nanomaterials in electrochemical enzyme biosensors, *Sensors* 9 (2009) 8547–8561.

[37] H. S. Z. A. Munir, J. Wang, Dynamics of capturing process of multiple magnetic nanoparticles in a flow through microfluidic bioseparation system, *IEEE Trans. Nanobiotechnol.,* 3 (2009) 55–64.

[38] D. Huh, B. D. Matthews, A. Mammoto, M. Montoya-Zavala, H. Y. Hsin, D. E. Ingber, Reconstituting organ-level lung functions on a chip, *Science* 328 (5986) (2010) 1662–1668.

[39]A.Kuznetsov,Theonsetofnanofluidbioconvectioninasuspensioncontainingbothnanoparticl esandgyrotacticmicroorganisms,*International Communications in Heat and Mass Transfer,* 37 (10) (2010) 1421 – 1425.

[40] A. Kuznetsov, D. Nield, Double-diffusive natural convective boundary-layer flow of a nanofluid past a vertical plate, *International Journal of Thermal Sciences* 50 (5) (2011) 712 – 717.

[41] A. Aziz, W. Khan, I. Pop, Free convection boundary layer flow past a horizontal flat plate embedded in porous medium filled by nanofluid containing gyrotactic microorganisms, *International Journal of Thermal Sciences* 56 (2012) 48 – 57.

[42] W. A. Khan, O. Makinde and Z. Khan, MHD boundary layer flow of a nanofluid containing gyrotactic microorganisms past a vertical plate with Navier slip, International Journal Heat and Mass Transfer, 74 (2014) 285–291.

[43] M.J. Uddin, W.A. Khan, and O. Anwar Bég, Bioconvection nanofluid slip flow past a wavy surface with applications in nano-biofuel cells *Chin. J. Physics,* 55, 2048-2063 (2017).

[44] N. A. Latiff, M. J. Uddin, O. Anwar Bég and A. I. M. Ismail, Unsteady forced bioconvection slip flow of a micropolar nanofluid from a stretching/ shrinking sheet, *Proc. IMECHE- Part N: J. Nanoengineering and Nanosystems,* 230 (4) 177–187 (2016).

[45] K. Das *et al.,* Nanofluid bioconvection in presence of gyrotactic microorganisms and chemical reaction in a porous medium, *J. Mechanical Science and Technology,* 29, 4841–4849 (2015).

[46] S. Shaw *et al.,* Magnetohydrodynamics and Soret effects on bioconvection in a porous medium saturated with a nanofluid containing gyrotactic microorganisms, *ASME J. Heat Transfer,* 136(5), 052601 (2014).

[47] Q. Zhao *et al.,* Unsteady bioconvection squeezing flow in a horizontal channel with chemical reaction and magnetic field effects, *Mathematical Problems in Engineering,* Volume 2017, Article ID 2541413, 9 pages (2017).

[48] O. Anwar Bég, M. Faisal Md Basir, M.J. Uddin, and A. I. Md. Ismail, Numerical study of slip effects on asymmetric bioconvective nanofluid flow in a porous microchannel with an expanding/contracting upper wall using Buongiorno's model, *J. Mechanics in Medicine and Biology*, 17 (5) 1750059 (2017).

[49] W. N. Mutuku, O. D. Makinde, Hydromagnetic bioconvection of nanofluid over a permeable vertical plate due to gyrotactic microorganisms, *Computers & Fluids*, 95 (2014) 88 – 97.

[50] O. Anwar Bég, Md. Jashim Uddin and W.A. Khan, Bioconvective non-Newtonian nanofluid transport in porous media containing micro-organisms in a moving free stream, *J. Mechanics Medicine Biology,* 15, 1550071.1-1550071.20 (2015).

[51] J.J. Li *et al.*, Unsteady mixed bioconvection flow of a nanofluid between two contracting or expanding rotating discs, *Zeitschrift für Naturforschung A,* 71, 1-12 (2017).

[52] S. Zhang and D. Zhao, *Advances in Magnetic Materials: Processing, Properties, and Performance,* 748 pages, CRC Press, Florida, USA (2017).

[53] G. Xu *et al.,* Experimental thermal evaluation of a novel solar collector using magnetic nano-particles, *Energy Conversion and Management,* 130, 252-259 (2016).

[54] S. A. M. Mehryan, F. Moradi Kashkooli, M. Soltani, K. Raahemifar, Fluid flow and heat transfer analysis of a nanofluid containing motile gyrotactic micro-organisms passing a nonlinear stretching vertical sheet in the presence of a non-uniform magnetic field; numerical approach, *Plos One* 11 (6) (2016) 1–32.

[55] B. Gebhart, Effects of viscous dissipation in natural convection, *J. Fluid Mechanics*, 14, 225 – 232 (1962).

[56] M.A. Alghoul, M.Y. Sulaiman, B.Z. Azmi and M.Abd. Wahab, Review of materials for solar thermal collectors, *Anti-Corrosion Methods and Materials*, 52/4 (2005) 199–206.

[57] C. A. Charitidis *et al.*, Manufacturing nanomaterials: from research to industry, *Manufacturing Rev.*, 11, 1-19 (2014).

[58] T. Thumma, O. Anwar Bég and Siva Reddy Sheri, Finite element computation of transient dissipative double-diffusive magneto-convective nanofluid flow from a rotating vertical porous

surface in porous media, *Proc. IMechE- Part N– J. Nanoengineering Nanomaterials and Nanosystems,* 231, 89–108 (2017).

[59] Nisha Shukla, Puneet Rana, O. A. Bég, and Bani Singh, Effect of chemical reaction and viscous dissipation on MHD nanofluid flow over a horizontal cylinder: Analytical solution, *AIP Conf. Proc.-Mathematical Sciences and its Applications,* 1802, 020015-1–020015-7 (2017).

[60] M.K. Nayak, MHD 3D flow and heat transfer analysis of nanofluid by shrinking surface inspired by thermal radiation and viscous dissipation, *International Journal of Mechanical Sciences,* 124/125, 185-193 (2017).

[61] Shu, C., Y. T. Chew, and B. E. Richards, Generalized differential-integral quadrature and their application to solve boundary layer equations, *Int. J. Numer. Methods Fluids,* 21, 723–733 (1995).

[62] T. Chiam, Hydromagnetic flow over a surface stretching with a power-law velocity, *International Journal of Engineering Science,* 33 (3) (1995) 429 – 435.

[63] P. Rana, R. Bhargava, Flow and heat transfer of a nanofluid over a nonlinearly stretching sheet: A numerical study, *Communications in Nonlinear Science and Numerical Simulation* 17 (1) (2012) 212 – 226.

[64] W. N. Mutuku, O. D. Makinde, Hydromagnetic bioconvection of nanofluid over a permeable vertical plate due to gyrotactic microorganisms, *Computers & Fluids* 95 (2014) 88 – 97.

[65] R. Bhargava, O. Anwar Bég, S. Sharma, J. Zueco, Finite element study of nonlinear two-dimensional deoxygenated biomagnetic micropolar flow, *Commun Nonlinear Sci Numer Simulat,* 15, 1210–1223 (2010).

[66] R. Bhargava, S. Sharma, H. S. Takhar, O. Anwar Bég, P. Bhargava, Numerical solutions for micropolar transport phenomena over a nonlinear stretching sheet, *Nonlinear Analysis: Modelling and Control*, 12(1), 45- 63 (2008).

[67] W. Khan, I.Pop, Boundary-layer flow of a nanofluid past a stretching sheet, *International Journal of Heat and Mass Transfer*, 53 (2010) 2477 – 2483.

[68] O. Anwar Bég, Numerical methods for multi-physical magnetohydrodynamics, Chapter 1, pp. 1-112, *New Developments in Hydrodynamics Research, M. J. Ibragimov and M. A. Anisimov, Eds., Nova Science, New York,* September (2012).

[69] C. Shu, *Differential Quadrature and Its Application in Engineering*, Springer, Berlin (2000).

[70] Tasveer A. Bég, GDQ and BEM simulation in earthquake magnetic and viscoelastic damping systems, Technical Report Sesimic A31-B, *Computational Mechanics and Renewable Energy Consultants,* Manchester, UK, 124 pp, December (2017).